

Enhanced One-Loop Corrections to WIMP Annihilation and their Thermal Relic Density in the Coannihilation Region

Manuel Drees ^{*} and Jie Gu [†]

*Physikalisches Institut and Bethe Center for Theoretical Physics,
Universität Bonn, Nussallee 12, 53115 Bonn, Germany*

Abstract

We consider quantum corrections to co-annihilation processes of Weakly Interacting Massive Particles (WIMPs) due to the exchange of light bosons in the initial state (“Sommerfeld corrections”). We work at one-loop level, i.e. we assume that these corrections can be treated perturbatively. Co-annihilation is important if there is at least one additional new particle with mass close to the lightest WIMP, which is a Dark Matter candidate. In this case the exchange of a (relatively light) boson in the initial state can change the identity of the annihilating particles. The corrections we are interested in factorize, as in the case of WIMP self-annihilation treated previously, but they can mix different tree-level amplitudes. Moreover, even small mass splittings between the external particles and those in the loop can change the relevant loop functions significantly. We find exact analytical expressions for these functions, and illustrate the effects by considering the cases of wino- or higgsino-like neutralinos as examples.

arXiv:1301.1350v2 [hep-ph] 15 Mar 2013

^{*}drees@th.physik.uni-bonn.de

[†]jiegu@th.physik.uni-bonn.de

1 Introduction

Decades after the discovery of the first hint of the existence of Dark Matter, still little is known about its nature. The perhaps best motivated Dark Matter candidates are “weakly interacting massive particles” (WIMPs), since they automatically have the roughly correct relic density if they are produced thermally within standard cosmology. These particles would have decoupled from the thermal plasma at a temperature of about 5% of their mass, when they were already quite non-relativistic. Their relic density scales inversely with the total (effective) WIMP annihilation cross section. Precise predictions for the relic density, with an error similar to or smaller than that of current or near-future determinations of the overall Dark Matter density from cosmological observations, therefore require precise calculations of the relevant annihilation cross sections. Right now the best observational constraint on the Dark Matter relic density comes from the combination of data from the WMAP satellite, type Ia supernovae, and the baryon acoustic oscillation (BAO), which gives [1]

$$\Omega_{\text{CDM}}h^2 = 0.1131 \pm 0.0034, \quad (1)$$

where h is the scaled Hubble parameter defined by $H_0 = 100h \text{ km s}^{-1}\text{Mpc}^{-1}$. Data from the PLANCK satellite should soon reduce the error to about 1.5%. Accordingly, on the theory side at least leading loop corrections to the annihilation cross section of WIMPs should be calculated to attain a percentage level precision.

One class of potentially large loop corrections is due to long range interactions between the WIMPs before their annihilation, mediated by the exchange of a boson with mass well below the WIMP mass. Consider two WIMPs with mass m_χ coming to a head-on point-like annihilation. Each WIMP can be described by a plane wave function. In the classical limit the exchange of a boson ϕ with coupling parameter α before the annihilation produces a potential, which is Coulomb-like if ϕ is massless or Yukawa-like otherwise. If the Bohr radius $1/(\alpha m_\chi)$ is smaller than the interaction range $1/m_\phi$, the plane wave functions are significantly deformed within the potential. As a consequence the annihilation cross section is enhanced (suppressed) in the case of an attractive (repulsive) potential. The magnitude of the correction depends on the strength of the potential. The larger the Bohr energy of the potential $\alpha^2 m_\chi/2$ is compared to the kinetic energy $m_\chi v^2/2$ of the dark matter particle, the larger is the correction to the cross section. If both conditions are satisfied, i.e. $\alpha m_\chi/m_\phi \gtrsim 1$ (radius condition) and $v \lesssim \alpha$ (energy condition), the correction to the cross section is so strong that the perturbative expansion breaks down and one has to solve the Schrödinger equation with the potential to compute the deformation of the wave functions [2, 3, 4].

However, the radius condition $\alpha m_\chi/m_\phi \gtrsim 1$ can raise naturalness issues in any extension of the Standard Model of particle physics that aims to ease the hierarchy problem. In the Minimal Supersymmetric extension of the SM (MSSM), for example, this condition can hardly be realized if ϕ is a weak gauge or Higgs boson. In the most natural case, with the mass of $\tilde{\chi}_1^0 \lesssim 1 \text{ TeV}$ and the weak coupling $\alpha_W \sim 1/30$, $\alpha m_\chi/m_\phi$ is still smaller (but not necessarily much smaller) than one. A one-loop calculation, which can be performed analytically, should then still produce a reasonably good approximation to the “exact” cross section based on a fully non-perturbative calculation.

This paper builds on ref. [5], where enhanced one-loop corrections to WIMP self-annihilation were treated. We extend these results to the co-annihilation region where the WIMP sector

includes several particles with masses close to that of the lightest WIMP. This, e.g., occurs naturally if the Dark Matter particle is part of a non-trivial multiplet of some non-abelian gauge group, which is broken at a scale somewhat smaller than the WIMP mass. This situation is considerably more complex than that treated in ref. [5]. On the one hand, co-annihilation between the lightest WIMP and one of its slightly heavier siblings has to be included, along with annihilation of the heavier states; the Sommerfeld-enhanced one-loop corrections will in general be different for these different initial states. Moreover, the exchange of a boson in the initial state can change the identity of the annihilating particles, as illustrated in Fig. 1. Even in the usual non-relativistic approximation, where the corrections factorize at the amplitude level, the one-loop correction to a given annihilation amplitude can therefore be proportional to a *different* tree-level annihilation amplitude. This means that the corrections no longer factorize at the cross section level, and signs – or, more generally, phases – between tree-level annihilation amplitudes with the same final state but different initial states become relevant.

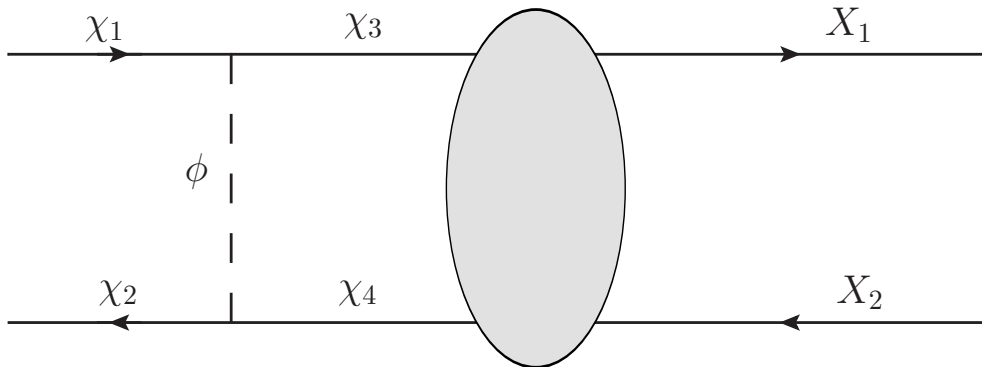


Figure 1: One loop correction to the annihilation of the WIMPs $\chi_1\chi_2$. They change into a new particle pair $\chi_3\chi_4$ after the exchange of boson ϕ . The four dark fermions χ_i , ($i = 1, \dots, 4$) may or may not be different states, but we assume them to be close in mass.

In this paper we obtain general analytical formulas for the one loop ‘‘Sommerfeld’’ correction, allowing all four masses before and after the boson exchange to be (slightly) different; this makes the use of the fitting formulae of ref. [5] unnecessary. We will see that the mass splitting is relevant unless $|\delta m|m_\chi \ll m_\phi^2$, where m_ϕ is the mass of the exchanged boson. A finite mass splitting can even enhance the size of the corrections, if the particles in the loop are somewhat heavier than the external particles; this agrees with results of ref. [6], where purely off-diagonal couplings to an ‘‘excited WIMP’’ were treated in the non-perturbative regime. As usual, we treat annihilation from S - and P -wave initial states separately; the resulting correction factors differ whenever the exchanged boson has a non-vanishing mass.

Our results are applicable to any co-annihilation process in any model. Two concrete sample calculations are given in the framework of the MSSM, and the corresponding corrections to the relic density are shown. This complements refs. [2, 7, 8], where these corrections were computed in the non-perturbative regime, i.e. for wino-like neutralinos with masses well above 1 TeV.

The remainder of the paper is organized as follows. Section 2 introduces the generalized formalism based on [5] and gives the model-independent analytical expressions for the correction factors at the amplitude level. We also point out that the exchange of fermions, which can

occur if the co-annihilating WIMPs have different spin, does *not* lead to enhanced corrections. Section 3 discusses some properties of the solutions. In Section 4 we apply these results to two MSSM scenarios. The last Section summarizes.

2 Formalism

Consider the general one-loop process depicted in Fig. 1, involving the exchange of a relatively light boson ϕ between two fermions in the initial state and two possibly different fermions in the intermediate state:

$$\chi_1 + \chi_2 \xrightarrow[\text{exch.}]{\phi} \chi_3 + \chi_4 \xrightarrow{\text{ann.}} X + Y. \quad (2)$$

We will assume that all four fermions¹ are close in mass to the lightest WIMP, which is a Dark Matter candidate. X and Y in the final state are standard model particles. We are interested in computing the annihilation cross sections during and after the decoupling of the WIMPs from the plasma of SM particles. Since decoupling occurs at temperature $T \sim m_\chi/20$, an expansion of all relevant amplitudes in terms of the relative velocity v , or of the three-momentum \vec{p} of the annihilating particles in the center-of-mass system (cms), in most cases [9] converges reasonably fast. The annihilation amplitude can be decomposed into partial waves, and only the leading S - and P -wave contributions are important, which start at order $|\vec{p}|^0$ and $|\vec{p}|^1$, respectively.

We are interested in scenarios where the boson mass m_ϕ is significantly smaller than the typical WIMP mass m_χ . The dominant contribution to the loop amplitude then comes from configurations where the virtual momentum carried by ϕ is much smaller than the momentum exchanged in the $\chi_1\chi_2$ annihilation; this allows the fermions χ_3 and χ_4 after rescattering to still be non-relativistic and almost on-shell if their masses are close to those of the fermions in the initial state, thereby enhancing the loop correction. Besides, the small loop momentum \vec{q} enables the factorization of the exchange of the boson ϕ before the annihilation, which significantly simplifies the calculation, as we will see later. Since in the non-relativistic approximation the loop correction is UV finite, no renormalization is required.

Given the initial momenta p_1, p_2 and the final momenta p'_1, p'_2 , following ref.[4] we introduce the four-vectors $P = (p_1 + p_2)/2$, half the total momentum, and $p = (p_1 - p_2)/2$ whose spatial component is the three-momentum of the annihilating fermion χ_1 in the cms. In this frame, P and p are explicitly given by,

$$P_0 = (\sqrt{\vec{p}^2 + m_1^2} + \sqrt{\vec{p}^2 + m_2^2})/2, \quad \vec{P} = 0, \quad (3)$$

and,

$$p_0 = (\sqrt{\vec{p}^2 + m_1^2} - \sqrt{\vec{p}^2 + m_2^2})/2. \quad (4)$$

The momentum difference in the final state, $p' = (p'_1 - p'_2)/2$, affects the annihilation amplitude, but it is irrelevant for the calculation of the correction.

¹As in ref. [5], the final result holds for bosonic WIMPs as well.

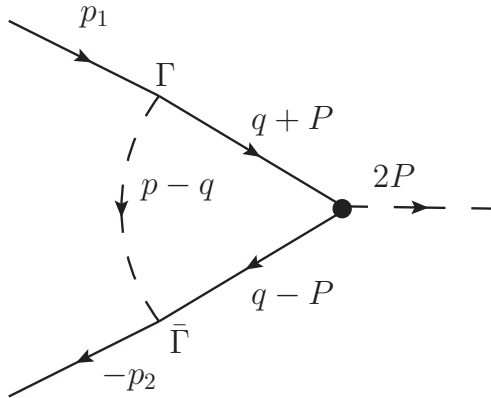


Figure 2: Feynman diagram for calculating the amplitude correction $\delta A_L(|\vec{p}|, p')$. $P = (p_1 + p_2)/2$, $p = (p_1 - p_2)/2$, and q is the loop momentum. The coupling matrices Γ and $\bar{\Gamma}$ are 1 for scalar coupling, and the big blob represents the $\chi_3\chi_4$ annihilation vertex.

Following the line of the argument in ref. [5], the one-loop correction term to the annihilation amplitude can be written as,

$$\delta A_L^{X_1 X_2}(|\vec{p}|, p') = ig_{\phi\chi_1\chi_3} g_{\phi\chi_2\chi_4}^* \bar{v}(p_2) \int \frac{d^4 q}{(2\pi)^4} \frac{\Gamma(\not{q} - \not{P} + m_4)(\gamma_5)^{n_L}(\not{q} + \not{P} + m_3)\bar{\Gamma}}{[(q - P)^2 - m_4^2 + i\epsilon][(q + P)^2 - m_3^2 + i\epsilon]} \times \frac{1}{[(p - q)^2 - m_\phi^2 + i\epsilon]} \tilde{A}_{0,L}^{X_3 X_4}(|\vec{q}|, p') u(p_1). \quad (5)$$

Here m_i , $i \in \{1, 2, 3, 4\}$ is the mass of fermion χ_i , and q is the loop momentum as illustrated in Fig.2. The matrices Γ and $\bar{\Gamma}$ describe the $\phi\bar{\chi}_3\chi_1$ and $\phi\bar{\chi}_2\chi_4$ couplings, whose strengths are given by the (possibly complex) couplings $g_{\phi\chi_i\chi_j}$. For scalar, pseudoscalar, vector, and axial vector couplings, Γ and $\bar{\Gamma}$ are $(\mathbf{1}, \mathbf{1})$, (γ_5, γ_5) , (γ^μ, γ_μ) , and $(\gamma^\mu\gamma_5, \gamma_\mu\gamma_5)$ (index μ is summed over), respectively. In the latter two cases, an extra overall minus sign should be introduced, coming from the propagator of the spin-1 boson ϕ . $(\gamma_5)^{n_L}$ (more on this later) stands for the effective Lorentz structure of the annihilation process; the remaining dynamics of the annihilation is contained in the “reduced” amplitude $\tilde{A}_{0,L}^{X_3 X_4}(|\vec{q}|, p')$.

As in [5] the “switch” $(\gamma_5)^{n_L}$ serves to differentiate between S - ($n_L = 1$) and P -wave ($n_L = 0$) contributions, though an explanation of its validity in the extended scenario here is in order. In the previous work [5] the annihilating particles were assumed to be identical Majorana fermions. In this case the Pauli exclusion principle only allows one choice of the total spin S for each partial wave, and the CP parity of the initial state is fixed. Here the initial particles can be different fermions. The total spin S is then no longer determined uniquely by the orbital angular momentum L , i.e. by the partial wave considered. In general all the possibilities listed in Table 1 need to be considered.

However we can opt to focus on the $J = 0$ configuration as representative for a given partial wave, i.e. the 1S_0 state in the S -wave and 3P_0 state in the P -wave. This can be described by a scalar-like effective vertex, i.e. the $(\gamma_5)^{n_L}$ Lorentz structure, including both scalar ($n_L = 0$) and pseudoscalar ($n_L = 1$) types, to describe the annihilation of WIMPs. Here one is exploiting the fact that the complicated three-momentum dependence of the Sommerfeld enhancement

	$S = 0$	$S = 1$
$L = 0$	1S_0	3S_1
$L = 1$	1P_1	$^3P_0, ^3P_1, ^3P_2$

Table 1: Possible spin states in each partial wave. For each state labeled by $^{2S+1}L_J$, S is the total spin, L the orbital angular momentum (partial wave), and J is the total angular momentum.

depends only on the partial wave type, i.e. it is independent of S and J .²

A noteworthy feature of Eq.(2) is the mixing between different channels. $\delta A_L^{\chi_1\chi_2}$ is the correction to the amplitude $A_L^{\chi_1\chi_2}$ of the annihilation of a $\chi_1\chi_2$ pair, while $\tilde{A}_{0,L}^{\chi_3\chi_4}$ on the right-hand side is the “reduced” tree-level amplitude for $\chi_3\chi_4$ annihilation. As a result we can no longer hope to factorize the correction at the cross section level, unlike in ref.[5]. This considerably complicates the calculation of these corrections in actual applications, as we will demonstrate in the sample calculations of Section 4.

We simplify Eq.(2) using the same approximations as in ref.[5]. First, the \vec{q} dependence in the “reduced” bare amplitude $\tilde{A}_{0,L}^{\chi_3\chi_4}$ is neglected in the non-relativistic limit. This allows to pull the bare amplitude $\tilde{A}_{0,L}^{\chi_3\chi_4}$ out of the integral, i.e. factorization still works at the amplitude level. The bosonic propagator, $1/[(p-q)^2 - m_\phi^2]$, is approximated by the instantaneous “Coulomb-like” part, $-1/[(\vec{p}-\vec{q})^2 + m_\phi^2]$, since in the non-relativistic limit the energy exchange is much smaller than the momentum exchange. The rest of the denominator has two poles beneath the real axis of q^0 , situated at $\omega_4 + P^0 - i\epsilon$ and $\omega_3 - P^0 - i\epsilon$, where $\omega_{3,4} = \sqrt{\vec{q}^2 + m_{3,4}^2}$. The first pole gives a much larger denominator and its residual is neglected. The denominator of the residue of the second pole is:

$$\begin{aligned} \mathcal{D} &= \frac{m_3 + m_4}{m_4} \cdot (m_1 + m_2 - m_3 + m_4) \cdot \vec{p}^2 \\ &\times \left[\frac{\vec{q}^2}{\vec{p}^2} - \frac{m_3 m_4}{m_3 + m_4} \frac{m_1 + m_2}{m_1 m_2} + \frac{2m_3 m_4}{m_3 + m_4} \frac{1}{\vec{p}^2} (m_3 + m_4 - m_1 - m_2) \right] \\ &\times [(\vec{p} - \vec{q})^2 + m_\phi^2]. \end{aligned} \quad (6)$$

Here we have performed non-relativistic expansions of all energies, keeping only the leading non-vanishing powers of \vec{p}^2 and \vec{q}^2 . Defining two auxiliary parameters,

$$c_D = \frac{m_3 + m_4}{m_4} \cdot (m_1 + m_2 - m_3 + m_4), \quad (7)$$

$$\kappa = \frac{m_3 m_4}{m_1 m_2} \frac{m_1 + m_2}{m_3 + m_4} - \frac{2m_3 m_4}{m_3 + m_4} \frac{1}{\vec{p}^2} (m_3 + m_4 - m_1 - m_2), \quad (8)$$

Eq.(6) can be written in a succinct way, regardless of the partial wave,

$$\mathcal{D} = c_D \cdot \vec{p}^2 \cdot \left[\frac{\vec{q}^2}{\vec{p}^2} - \kappa \right] [(\vec{p} - \vec{q})^2 + m_\phi^2]. \quad (9)$$

²We will see later that the sign and strength of the Sommerfeld correction can also depend on S and J ; here we wish to compute the loop functions describing the non-trivial dynamics of the corrections, which depend only on L .

The numerator of Eq.(2) differs for the two partial waves we are considering. In case of S -wave annihilation, $n_L = 1$. In this case we can set all 3-momenta in the numerator to zero. Moreover, since we can get an enhanced correction only if all four participating fermions χ_i have similar masses, we ignore terms $\propto (m_1 - m_2)(m_3 - m_4)$ which is of second order in mass differences. Performing a string of gamma matrix algebra, the Lorentz structure of the numerator

$$\mathcal{N} := \bar{v}(p_2)\Gamma(\not{q} - \not{P} + m_4)(\gamma_5)^{n_L}(\not{q} + \not{P} + m_3)\bar{\Gamma}u(p_1) \quad (10)$$

is reduced to

$$\mathcal{N} = c_N^S \bar{v}(p_2)\gamma_5 u(p_1). \quad (11)$$

The coefficient c_N^S depends on the types of $\phi\chi_1\chi_3$ and $\phi\chi_4\chi_2$ vertices:

$$c_N^S = \begin{cases} (m_1 + m_2)^2/4 + m_3m_4 + (m_1 + m_2)(m_3 + m_4)/2, & \text{scalar} \\ -(m_1 + m_2)^2/4 - m_3m_4 + (m_1 + m_2)(m_3 + m_4)/2, & \text{pseudoscalar} \\ (m_1 + m_2)^2 + 4m_3m_4 - (m_1 + m_2)(m_3 + m_4), & \text{vector} \\ -[(m_1 + m_2)^2 + 4m_3m_4 + (m_1 + m_2)(m_3 + m_4)]. & \text{axial vector} \end{cases} \quad (12)$$

Here for vector and axial vector couplings the negative sign in the propagator has been absorbed into c_N^S . If we write $m_{2,3,4} = m_1(1 + \epsilon_{2,3,4})$ and expand up to linear order in the mass differences described by the ϵ_i , the results for the scalar and vector are the same, being given by $4m_1^2 [1 + (\epsilon_2 + \epsilon_3 + \epsilon_4)/2]$; the result for the axial vector exchange differs from that for vector exchange by a factor of -3 [5], whereas c_N^S for pseudoscalar interaction is of order ϵ^2 , and can thus be neglected to the order we are interested in.

The bi-spinor in \mathcal{N} remains finite as $|\vec{p}| \rightarrow 0$, as expected for an S -wave amplitude. It can be combined with the reduced amplitude to give the full tree-level $\chi_3\chi_4$ annihilation amplitude. The correction for the S -wave $\chi_1\chi_2$ annihilation amplitude is therefore proportional to the tree $\chi_3\chi_4$ annihilation amplitude,

$$\delta A_S^{\chi_1\chi_2}(|\vec{p}|, p')|_{1\text{-loop}} = \frac{g_{\phi\chi_1\chi_3}g_{\phi\chi_2\chi_4}^*}{8\pi^2} \frac{c_N^S}{c_D|\vec{p}|} \sqrt{\frac{m_1m_2}{m_3m_4}} I_S(r, \kappa) A_{0,S}^{\chi_3\chi_4}(|\vec{p}|, p'), \quad (13)$$

where the universal numerical prefactors to the numerator and denominator c_N^S , c_D are given by Eq.(12) and Eq.(7), respectively. The square root in front of I_S occurs because in Eq.(11) the external fermions are χ_1 and χ_2 , whereas the amplitude $A_{0,S}^{\chi_3\chi_4}$ obviously refers to reactions with χ_3 and χ_4 in the initial state; in the relevant non-relativistic limit, the spinors simply reduce to the square root of the mass of the respective fermion. Finally, the function $I_S(r, \kappa)$ describing the dynamics of the correction is defined as

$$I_S(r, \kappa) = \Re \left[\int_0^\infty \frac{x}{x^2 - \kappa} \ln \frac{(1+x)^2 + r}{(1-x)^2 + r} dx \right]. \quad (14)$$

κ has been defined in Eq.(8), and r is given by

$$r = \frac{m_\phi^2}{|\vec{p}|^2}. \quad (15)$$

Note that the integral in Eq.(14) should be understood as a principal value integral.

Before evaluating the integral in Eq.(14), we discuss the case of P -wave annihilation, which corresponds to $n_L = 0$. Here we again neglect terms that are of second or higher order in fermion mass differences, but we keep terms linear in the 3-momenta \vec{p} , \vec{q} . Similar algebra as for S -wave annihilation shows that the numerator is proportional to $\bar{v}(p_2) (a_\Gamma \not{q} + b_\Gamma) u(p_1)$, where the constants a_Γ and b_Γ depend on the Dirac structure of the $\phi\chi_i\chi_j$ couplings. Note that both terms are of first order in the three-momentum: \not{q} is explicitly of this order, but the γ matrix couples the two large spinor components, as can easily be seen in Dirac representation. The second term is $\mathcal{O}(\vec{p})$ since the bi-spinor only contains products of one large and one small spinor component. The term proportional to b_Γ , which vanishes for vanishing mass splitting between the four fermions, can be treated straightforwardly. Since in a one-loop calculation we need the interference between the one-loop amplitude and the tree-level amplitude, we treat the term $\propto a_\Gamma$ by multiplying the one-loop correction with the hermitean conjugate of the tree-level amplitude $\bar{v}(p_2)u(p_1)$, and dividing by the square of the tree-level amplitude. In other words, we replace the one-loop amplitude $\delta A_{1,P}$ by $(\delta A_{1,P} A_{0,P}^\dagger) A_{0,P}/|A_{0,P}|^2$, which leaves the relevant product $\delta A_{1,P} A_{0,P}^\dagger$ unchanged. This yields:

$$\mathcal{N} \cdot \tilde{A}_{0,L}^{\chi_3, \chi_4} = \left(d_N^P + c_N^P \cdot \frac{\vec{q} \cdot \vec{p}}{\vec{p}^2} \right) A_{0,L}^{\chi_3, \chi_4}, \quad (16)$$

where the numerical factors c_N^P , d_N^P are

$$c_N^P = \begin{cases} 2 \frac{m_1 m_2}{m_1 + m_2} (m_1 + m_2 + m_3 + m_4), & \text{scalar} \\ 2 \frac{m_1 m_2}{m_1 + m_2} (m_3 + m_4 - m_1 - m_2), & \text{pseudoscalar} \\ 4 \frac{m_1 m_2}{m_1 + m_2} (m_3 + m_4), & \text{vector} \\ 4 \frac{m_1 m_2}{m_1 + m_2} (m_3 + m_4), & \text{axial vector} \end{cases} \quad (17)$$

$$d_N^P = \begin{cases} m_3 m_4 - (m_1 + m_2)^2/4, & \text{scalar} \\ (m_1 + m_2)^2/4 - m_3 m_4, & \text{pseudoscalar} \\ 4m_3 m_4 - (m_1 + m_2)^2, & \text{vector} \\ (m_1 + m_2)^2 - 4m_3 m_4, & \text{axial vector} \end{cases} \quad (18)$$

The coefficients for vector and axial vector interactions again contain an extra factor of -1 from the sign of the spin-1 propagator. We note that the d_N^P are all of the same form, but differ by overall factors; they all vanish linearly for vanishing mass differences. To linear order in mass differences, c_N^P for vector and axial vector interactions is the same as c_N^S for scalar or vector interactions, but c_N^P for scalar interactions differs, and c_N^P for pseudoscalar interactions vanishes only linearly in mass differences. A very light pseudoscalar with off-diagonal couplings³ could therefore give significant corrections to co-annihilation.

³For pseudoscalar coupling, c_N^P and d_N^P vanish if the coupling is diagonal, in which case $m_3 = m_1$ and $m_4 = m_2$.

In the end, the P -wave amplitude correction can be written as

$$\delta A_P^{X_1 X_2}(|\vec{p}|, p')|_{1\text{-loop}} = \frac{g_{\phi\chi_1\chi_3} g_{\phi\chi_2\chi_4}^*}{8\pi^2} \left(\frac{d_N^P}{c_D |\vec{p}|} I_S(r, \kappa) + \frac{c_N^P}{c_D |\vec{p}|} I_P(r, \kappa) \right) \sqrt{\frac{m_1 m_2}{m_3 m_4}} A_{0,P}^{X_3 X_4}(|\vec{p}|, p'). \quad (19)$$

The square root factor occurs for the same reason as in eq.(13), and the function $I_P(r, \kappa)$ is defined as

$$I_P(r, \kappa) = \Re e \left\{ \int_0^\infty \frac{2x^2}{x^2 - \kappa} \cdot \left[-1 + \frac{x^2 + 1 + r}{4x} \ln \frac{(x+1)^2 + r}{(x-1)^2 + r} \right] dx \right\} \quad (20)$$

So far we have assumed that $\chi_3\chi_4$ annihilation proceeds through a (pseudo)scalar vertex. This describes annihilation from a state with total angular momentum $J = 0$. As noted earlier, if the initial state consists of two identical Majorana fermions, there is a one-to-one correspondence between orbital angular momentum L and spin S , such that $L = 0$ (S -wave) requires spin $S = 0$, and hence $J = 0$. However, we saw above that this need no longer be true for co-annihilation processes. We therefore repeated the S -wave calculation for the case that $\chi_3\chi_4$ annihilate through a γ^ν vertex. This describes annihilation from a $J = 1$ state. Only a space-like index, $\nu = k \in \{1, 2, 3\}$, gives a non-vanishing tree-level amplitude in the limit of vanishing three-momentum. We find that the coefficients c_N^S for scalar, vector or axial vector interaction of the exchanged boson are now all equal to c_N^S for scalar boson exchange and annihilation through a γ_5 vertex, as given in Eq.(12); the coefficient for pseudoscalar interaction again vanishes, up to terms that are quadratic in mass splittings. In particular, in this case *no* factor -3 appears for axial vector exchange. Note that $L = 0$ and $J = 1$ implies $S = 1$. This is consistent with the rescattering argument of ref.[5].

	scalar	pseudoscalar	vector	axial vector
spin singlet	1	0	1	-3
spin triplet	1	0	1	1

Table 2: c_S or $c_N/(c_D m_\chi)$ for different spin states of the initial fermion pairs with different boson-WIMP coupling types.

In the limit of vanishing mass splitting we can therefore write the overall factor $c_N/(c_D m_\chi)$ for either the S - or P -wave as shown in Table 2. This coefficient simply becomes 1 (0 for pseudoscalar exchange), except for the case of axial vector boson exchange in a spin-singlet ($S = 0$) state. We see that this coefficient is in fact determined by S , rather than by L and J . Again in the limit where the fermion mass splittings can be neglected everywhere *except* in the definition of κ appearing in the loop functions, the correction to the $\chi_1\chi_2$ annihilation amplitude can then be written as:

$$\delta A_L^{X_1 X_2}(|\vec{p}|, p')|_{1\text{-loop}} = c_S \frac{g_{\phi\chi_1\chi_3} g_{\phi\chi_2\chi_4}^*}{8\pi^2} \frac{m_\chi}{|\vec{p}|} I_L(r, \kappa) A_{0,L}^{X_3 X_4}(|\vec{p}|, p'), \quad (21)$$

where m_χ is the mass of the WIMP. Recall that we are interested in the calculation of perturbative one-loop corrections. We expect the overall magnitude of these corrections to be of the

order of at most 10 or 20%; for larger corrections, resummations will be necessary. Moreover, co-annihilation is important only for mass splittings below 10% or so; in fact, in our numerical examples we will encounter much smaller mass splittings, as relevant for the annihilation of higgsino- or wino-like states in the MSSM. Contributions of order $(\alpha/\pi)(\delta m/m_\chi)$ can then safely be neglected. On the other hand, Eq.(8) shows that the quantity κ appearing in the denominators of the loop functions will diverge for *any* finite mass splitting when the initial three-momentum $\vec{p} \rightarrow 0$. It is therefore important to take the mass splitting into account when computing κ .

Note that Eq.(21) is applicable also to the (co-)annihilation of bosonic WIMPs, with spin 0 or 1. This has been shown in [5] for WIMP self-annihilation, and remains true also for the more complicated situation discussed here.

We have found analytical expressions for the integrals $I_L(r, \kappa)$ using contour integral methods, as follows. In the S partial wave,

$$I_S(r, \kappa) = \begin{cases} C_S(r, \kappa), & \kappa > 0, \\ C_S(r, \kappa) + P_S(r, \kappa), & \kappa < 0, \end{cases} \quad (22)$$

where $C_S(r, \kappa)$ comes from the branch cut of the logarithm in Eq.(14):

$$C_S(r, \kappa) = \begin{cases} \pi \cdot \arctan\left(\frac{2\sqrt{r}}{\kappa - 1 + r}\right), & \kappa > -r + 1, \\ \pi \cdot \left(\arctan\left(\frac{2\sqrt{r}}{\kappa - 1 + r}\right) + \pi\right), & \kappa < -r + 1, \end{cases} \quad (23)$$

and $P_S(r, \kappa)$ is the residual at the pole $i\sqrt{-\kappa}$ when κ is negative,

$$P_S(r, \kappa) = \begin{cases} -\pi \cdot \arctan\left(\frac{2\sqrt{-\kappa}}{\kappa + 1 + r}\right), & \kappa > -r - 1, \\ -\pi \cdot \left(\arctan\left(\frac{2\sqrt{-\kappa}}{\kappa + 1 + r}\right) + \pi\right), & \kappa < -r - 1. \end{cases} \quad (24)$$

In the P partial wave,

$$I_P(r, \kappa) = \begin{cases} C_P(r, \kappa), & \kappa > 0, \\ C_P(r, \kappa) + P_P(r, \kappa), & \kappa < 0, \end{cases} \quad (25)$$

where $C_P(r, \kappa)$ comes from the branch cut of the logarithm in Eq.(20):

$$C_P(r, \kappa) = \pi \left[-\sqrt{r} + \frac{\kappa + 1 + r}{2} \cdot \begin{cases} \arctan\frac{2\sqrt{r}}{\kappa - 1 + r}, & \kappa > -r + 1 \\ \arctan\frac{2\sqrt{r}}{\kappa - 1 + r} + \pi, & \kappa < -r + 1 \end{cases} \right], \quad (26)$$

and $P_P(r, \kappa)$ is the residual at the pole $i\sqrt{-\kappa}$ when κ is negative,

$$P_P(r, \kappa) = -\pi \left[-\sqrt{-\kappa} + \frac{\kappa + 1 + r}{2} \cdot \begin{cases} \arctan\frac{2\sqrt{-\kappa}}{\kappa + 1 + r}, & \kappa > -r - 1 \\ \arctan\frac{2\sqrt{-\kappa}}{\kappa + 1 + r} + \pi. & \kappa < -r - 1 \end{cases} \right]. \quad (27)$$

We note that the “classical” Sommerfeld effect refers to the exchange of a massless boson (i.e., $r = 0$) between fermions of equal mass (i.e., $\kappa = 1$). In this case one simply has $I_S(0, 1) = I_P(0, 1) = \pi^2/2$. However, for $r \neq 0$ the corrections to S - and P -wave annihilation differ significantly, as we will see shortly.

2.1 Complications due to Fermion Flow and Spin

Our discussion so far assumed implicitly that “Dirac arrows” can be drawn consistently along the fermion line, allowing to directly read off the correct order of external spinors, propagators and vertex factors. This is always true in the SM, thanks to the “accidental” conservation of lepton and baryon numbers, but need not be true in extensions of the SM. In particular, “clashing arrows” frequently occur in supersymmetric extensions of the SM [10].

In our case these occur in particular in diagrams with Majorana fermions; an example is shown in Fig. 3. We use the convention of Denner [11] to systematically treat such Feynman diagrams. In this treatment one introduces an auxiliary fermion flow, which is continuous through the diagram, as shown in the right diagram of Fig. 3. This auxiliary fermion flow is used to write down the spinor chain for this diagram. In most cases the original vertex factors should be used; however, if the auxiliary fermion flow goes against the direction of the usual Dirac arrow on a given vector–fermion–fermion vertex, with Dirac structure γ_μ , then this vertex receives an additional minus sign.⁴ If this procedure changes the order of external spinors, the whole amplitude should be multiplied with -1 . This rule ensures that the direction one chooses for the auxiliary fermion flow is not relevant. Moreover, since the only modification required is a possible minus sign in front of the amplitude, the calculations in the main part of this Section are not affected. More details on this method, and several examples, can be found in ref.[11].

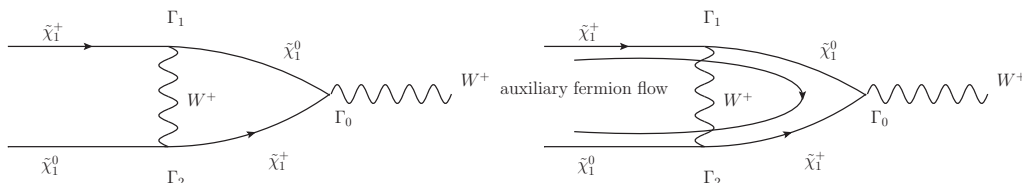


Figure 3: At the left is an example of a relevant Feynman diagram with clashing Dirac arrows, describing a one–loop correction to the s -channel annihilation of a chargino and a neutralino in a supersymmetric extension of the SM; here $\tilde{\chi}_1^+$ has been defined as “particle”, with Dirac arrow along the momentum direction. At the right is the same diagram with an (arbitrarily chosen) auxiliary, continuous fermion flow.

A second complication occurs when the products $g_{\phi\chi_1\chi_3}g_{\phi\chi_2\chi_4}$ and $g_{\phi\chi_1\chi_4}g_{\phi\chi_2\chi_3}$ are both nonzero and $\chi_3 \neq \chi_4$. In such cases there are two contributing Feynman diagrams where the intermediate particles are swapped; a pair of examples is shown in Fig. 4. In this case one needs to distinguish between $\chi_3\chi_4$ and $\chi_4\chi_3$ annihilation. Of course, at the level of cross sections these

⁴No such extra sign appears for axial vector vertices, with Dirac structure $\gamma_\mu\gamma_5$; the difference is due to the different behavior of these two Dirac structures when sandwiched with the appropriate combination of charge conjugation matrices [11].

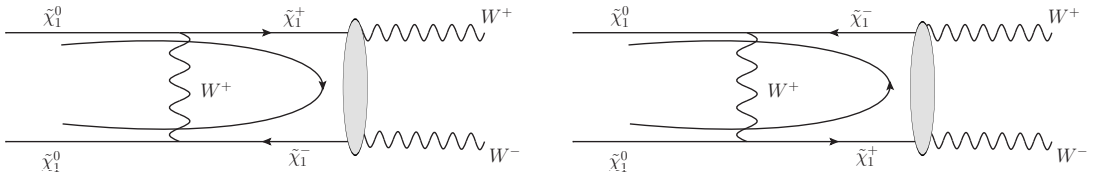


Figure 4: The annihilation of $\tilde{\chi}_1^0\tilde{\chi}_1^0$ with the intermediate state $\tilde{\chi}_1^+\tilde{\chi}_1^-$ can have two contributing Feynman diagrams. Again $\tilde{\chi}_1^+$ is a “particle”, i.e. $\tilde{\chi}_1^-$ is an “antiparticle” and has Dirac arrow opposite to the momentum direction. The auxiliary fermion flows are added in accordance with the Denner’s convention.

are the same (if consistent definitions of the scattering angle are used in both cases), but the corresponding amplitudes may differ by a sign. This sign can be determined as follows.

Let $\mathcal{A}(p, \cos\theta, \dots)$ be the reduced amplitude for $\chi_3\chi_4$ annihilation; here p is the absolute value of the cms three-momentum in the initial state, θ is the cms scattering angle, and \dots denotes possible other quantum numbers (e.g. the spin). The reduced amplitude of the “crossed” diagram, for $\chi_4\chi_3$ annihilation, is then given by $\mathcal{S}\mathcal{A}(p, -\cos\theta, \dots)$. The sign of $\cos\theta$ has to be changed since by convention the first annihilating particle has a fixed direction: if χ_3 goes in $+z$ direction in $\chi_3\chi_4$ annihilation, it goes in $-z$ direction in $\chi_4\chi_3$ annihilation. The overall sign \mathcal{S} depends on the spins involved. Note first of all that a crossed intermediate state only appears if all four χ_i obey the same statistics (Bose–Einstein or Fermi–Dirac).⁵ If they are fermionic, \mathcal{S} contains one factor of -1 from the crossing of fermion lines. An additional factor arises from the symmetry of the spin wave function⁶, if χ_3 and χ_4 are both spin- $1/2$ or spin- 1 particles. In the former case the spin wave function is symmetric for total spin $S = 1$ and antisymmetric for $S = 0$. If both χ_3 and χ_4 have spin 1, then the spin wave function is symmetric for $S = 0$ or 2, and antisymmetric for $S = 1$. Either way, an antisymmetric spin wave function leads to an additional -1 factor in \mathcal{S} . As a result, $\mathcal{S} = (-1)^S$ for the annihilation of either two spin- $1/2$ fermions or two spin- 1 bosons; however, the co-annihilation of one scalar and one vector boson always gives $\mathcal{S} = +1$.

2.2 Fermion Exchange

Before concluding this Section, we briefly comment on the exchange of light fermions between co-annihilating WIMPs. This is possible, e.g., in the co-annihilation of a supersymmetric neutralino and a slepton [12], where the exchanged fermion could be very light (a charged

⁵We will show in the next Subsection that the particle exchanged in the $\chi_1\chi_2 \rightarrow \chi_3\chi_4$ rescattering has to be a boson.

⁶The symmetry of the orbital angular momentum part of the wave function has already been described by the change of sign of $\cos\theta$.

fermion) or even nearly massless (a neutrino). Moreover, since the ‘‘Sommerfeld correction’’ is non-relativistic in nature, one might naively expect that exchange of a light fermion also leads to enhanced corrections; after all, the spin of the annihilating WIMPs does not matter in the usual Sommerfeld corrections.

However, one can see fairly easily that the exchange of a light fermion between (co-)annihilating WIMPs does *not* yield an enhanced correction. The reason is that the numerator of the fermion propagator contributes an extra factor $\not{p} - \not{q} + m_f$ to the numerator of the argument of the loop integral. Recall that \vec{q} has to be counted as being of order $|\vec{p}|$ here, and $q_0 \propto |\vec{p}|^2$. If the fermion is light, all three terms in this extra factor are therefore $\mathcal{O}(|\vec{p}|)$ or smaller; this implies that the correction will not be enhanced by a $1/v$ factor even for $m_f \rightarrow 0$. On the other hand, if m_f is comparable to the WIMP mass, this extra factor in the numerator does not give a significant suppression; however, in that case the loop integral is small, as general arguments in the Introduction indicate and the numerical results in the next Section show explicitly. Hence there is no range of m_f where one can expect an enhanced correction from fermion exchange. We therefore do not discuss these contributions any further.

3 Discussion of Results

The solutions Eq.(22) and Eq.(25) are two model-independent functions of variables r and κ only. In order to better understand the dependence of the size of the correction on r and κ , we define the amplitude enhancement function (\mathcal{E}_L),

$$\mathcal{E}_L(r, \kappa) := \frac{1}{2\pi} \sqrt{r} I_L(r, \kappa), \quad (28)$$

This allows to recast the the amplitude correction formula as:

$$\delta A_L^{\chi_1 \chi_2}(|\vec{p}|, p')|_{1\text{-loop}} = c_S \frac{\alpha m_\chi}{m_\phi} \mathcal{E}_L(r, \kappa) A_{0,L}^{\chi_3 \chi_4}(|\vec{p}|, p'), \quad (29)$$

where the relative enhancement of the annihilation amplitude simply consists of three parts: the uniform prefactor c_S given in Table 2, the one-loop factor $\alpha m_\chi / m_\phi$ with $\alpha = g_{\phi \chi_1 \chi_3} g_{\phi \chi_2 \chi_4}^* / (4\pi)$, and the amplitude enhancement function $\mathcal{E}_L(r, \kappa)$. Here and in the following numerical results we work to zeroth order in WIMP mass differences wherever possible, i.e. we set $m_1 = m_2 = m_3 = m_4 \equiv m_\chi$ everywhere *except* in the definition of κ , Eq.(8).

We first discuss several examples in order to illustrate the size of the radiative corrections we are calculating, and to understand the physics. We take 80 GeV (the mass of the W -boson) for the mass of the exchanged boson, and 1.1 TeV for the mass of the lightest among the four fermions (i.e. the dark matter particle); the latter is roughly the mass required by the thermal relic density today if the WIMP is a higgsino-like neutralino. Moreover, for simplicity we consider only two co-annihilating states. Since we are interested in situations with small mass splitting, $m_2 - m_1 \ll m_1$, we essentially have to consider only three processes.

The first reaction, $\chi_1 + \chi_1 \rightarrow \chi_1 + \chi_1 \xrightarrow{\text{ann.}} X + Y$, stands for all reactions where the fermion masses before and after rescattering are the same, i.e. these results are applicable (with very small changes) to any process of the kind $\chi_i \chi_j \rightarrow \chi_i \chi_j \xrightarrow{\text{ann.}} X + Y$. This is the case discussed

in [5]. Here $\kappa = 1$,⁷ so that

$$\mathcal{E}_S(r, \kappa = 1) = \frac{\sqrt{r}}{2} \cdot \arctan\left(\frac{2}{\sqrt{r}}\right), \quad (30)$$

$$\mathcal{E}_P(r, \kappa = 1) = \frac{\sqrt{r}}{2} \cdot \left[-\sqrt{r} + (1 + r/2) \arctan\left(\frac{2}{\sqrt{r}}\right) \right]. \quad (31)$$

The $\mathcal{E}_L(r, \kappa = 1)$ are plotted as functions of $|\vec{p}|$ for both the S - and P -wave in Fig. 5a. We see that \mathcal{E}_S saturates at 1 and \mathcal{E}_P^c saturates at $1/3$ in the zero-velocity limit, $|\vec{p}| \rightarrow 0$. For larger $|\vec{p}|$ \mathcal{E}_S remains larger than \mathcal{E}_P , but the two functions approach each other for large $|\vec{p}|$. Recall that $|\vec{p}| \gg m_\phi$ corresponds to $r \ll 1$, where $I_S(r, \kappa = 1)$ and $I_P(r, \kappa = 1)$ both approach $\pi^2/2$, i.e. in this limit $\mathcal{E}_S(r \ll 1, \kappa = 1) = \mathcal{E}_P(r \ll 1, \kappa = 1) \rightarrow \pi m_\phi / (4|\vec{p}|)$. We finally note that \mathcal{E}_P has a very broad maximum at $|\vec{p}| \simeq m_\phi/2$; however, the value at this maximum exceeds the value for $|\vec{p}| \rightarrow 0$ only by 6.8%. Nevertheless this maximum at non-vanishing $|\vec{p}|$ implies that \mathcal{E}_P remains approximately constant out to much larger momenta $|\vec{p}|$ than \mathcal{E}_S does.⁸

Next we consider the process where the particles in the intermediate states are heavier than the initial ones: $\chi_1 + \chi_1 \rightarrow \chi_2 + \chi_2 \xrightarrow{\text{ann.}} X + Y$, with $m_2 = m_1 + \delta m$. Since our correction function depend primarily on the total mass difference $m_i + m_j - m_k - m_l$, one finds very similar results for $\chi_1 \chi_1 \rightarrow \chi_1 \chi_2$ if the mass difference δm is doubled.

This case differs from the one we just discussed since now $\kappa \neq 1$ and is no longer a constant. Note that the entire dependence of the correction functions on the mass splitting is described by this parameter. For small mass splitting, $|\delta m| \ll m_1$, κ can be written as

$$\kappa \simeq 1 + \frac{\delta m}{m_1} \left(1 - \frac{2m_1^2}{\vec{p}^2} \right), \quad (32)$$

where $2\delta m$ is the difference between the sum of the masses in the initial state and the sum of the masses in the intermediate state; in the case at hand, $\delta m = m_2 - m_1$. In the limit $\vec{p} \rightarrow 0$, κ can be further simplified to

$$\kappa \simeq -\frac{\delta m}{m_1} \frac{2m_1^2}{\vec{p}^2}. \quad (33)$$

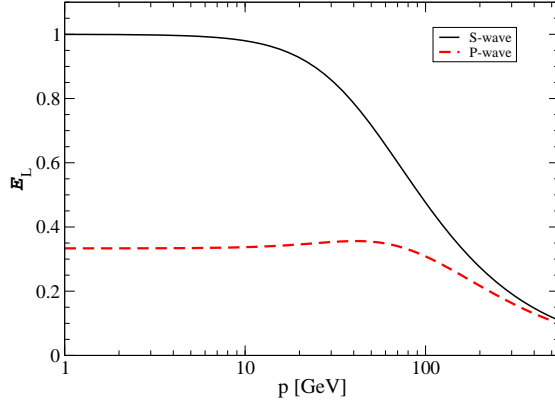
Note that for the reaction we are discussing, $\kappa \rightarrow -\infty$ as $|\vec{p}| \rightarrow 0$. Therefore even very small mass splittings have to be kept, if we want to describe the radiative corrections correctly at all values of $|\vec{p}|$.

The corresponding amplitude enhancement factors are plotted in Fig. 5b. Comparison with the first case discussed above shows that the correction still reaches a plateau as $|\vec{p}| \rightarrow 0$, albeit at a reduced value. This can be understood by expanding the functions $\mathcal{E}_L(r, \kappa)$ in terms of $\delta m/m$ in the limit $|\vec{p}| \rightarrow 0$. In the scenario we are considering, both the functions C_L given in Eqs.(23) and (26) and the functions P_L given in Eqs.(24) and (27) have to be included. This gives:

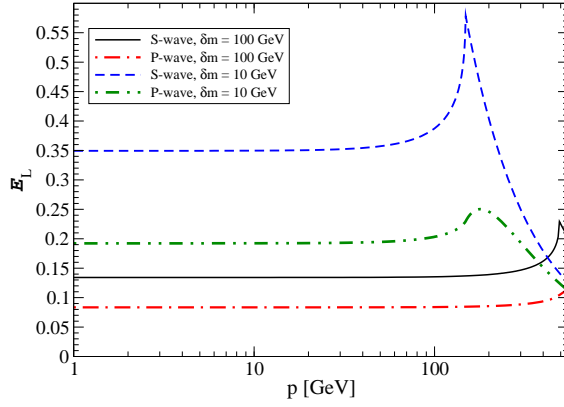
$$\mathcal{E}_S(r, \kappa)|_{|\vec{p}| \rightarrow 0} \simeq \frac{1}{1 + \sqrt{2 \frac{m_1 \delta m}{m_\phi^2}}}, \quad (34)$$

⁷In scenarios with three or more co-annihilating WIMPs it is possible to have rescatterings $\chi_i \chi_j \rightarrow \chi_k \chi_l$ such that $m_i + m_j = m_k + m_l$ but $m_i m_j \neq m_k m_l$, in which case κ is still independent of $|\vec{p}|$ but differs from 1.

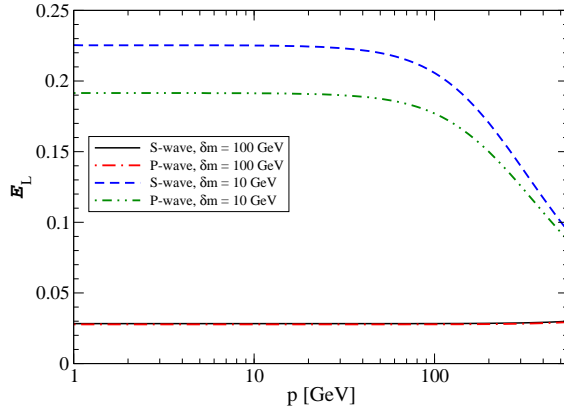
⁸This maximum is not reproduced by the numerical approximation of ref.[5].



(a) $\chi_1 + \chi_1 \rightarrow \chi_1 + \chi_1 \rightarrow X + Y$



(b) $\chi_1 + \chi_1 \rightarrow \chi_2 + \chi_2 \rightarrow X + Y$



(c) $\chi_2 + \chi_2 \rightarrow \chi_1 + \chi_1 \rightarrow X + Y$

Figure 5: The amplitude enhancement factors $\mathcal{E}_L(r, \kappa)$ are plotted as a function of $|\vec{p}|$ in the CM frame for the cases that the intermediate state is the same as the initial state (top), is heavier than the initial state (middle), and is lighter than the initial state (bottom); in the latter two cases, results for two different mass splittings are shown. These results are for a WIMP mass of 1.1 TeV and a boson mass of 80 GeV.

$$\mathcal{E}_P(r, \kappa)|_{|\vec{p}|\rightarrow 0} \simeq \frac{1}{3} \frac{1}{1 + \sqrt{2 \frac{m_1 \delta m}{m_\phi^2}}} \cdot \left(\frac{1 + 2 \sqrt{2 \frac{m_1 \delta m}{m_\phi^2}}}{1 + \sqrt{2 \frac{m_1 \delta m}{m_\phi^2}}} \right). \quad (35)$$

Note that $2m_1\delta m > m_\phi^2$ for all cases considered, leading to a sizable suppression of the correction, especially for S -wave annihilation. The suppression is less in the P -wave case because of the extra factor in parentheses.

Another characteristic feature of the curves in Fig. 5b is the occurrence of pronounced maxima at the threshold value of $|\vec{p}|$ where the intermediate state can be produced on-shell in non-relativistic kinematics. This happens at the point $|\vec{p}|^2 = 2m_1\delta m$, which corresponds to $\kappa = 0$. The S -wave function \mathcal{E}_S has a cusp at this point, i.e. is not differentiable, while \mathcal{E}_P as a function remains smooth at this maximum.

The physics is therefore clear. When $|\vec{p}|$ is below the threshold for real χ_2 pair production, the intermediate particles χ_2 are produced virtually and the correction is suppressed. At the threshold the intermediate state can finally be produced on-shell with zero relative velocity and the propagators of χ_2 in the one-loop correction are large. Afterwards the correction decreases again with increasing momentum. Note that for $|\vec{p}|$ values near the maximum, the loop correction for a heavier intermediate state can exceed that for diagonal scattering, i.e. for $\kappa = 1$, discussed above.

We finally discuss the case where the particles in the intermediate state are lighter than those in the initial state, i.e. $\chi_2 + \chi_2 \rightarrow \chi_1 + \chi_1 \xrightarrow{\text{ann.}} X + Y$. Again, results for $\chi_2\chi_2 \rightarrow \chi_1\chi_2$ are very similar, if the mass difference δm is increased by a factor of 2. The resulting loop functions $\mathcal{E}_L(|\vec{p}|)$ are plotted in Fig. 5c.

We again observe plateaus for $|\vec{p}| \rightarrow 0$. The finite mass splitting again leads to a suppression of the correction functions in this limit. Note that now $\kappa \rightarrow +\infty$ in this limit, so that the P_L functions of Eqs.(24) and (27) do not contribute. This leads to a stronger suppression than in the previous case where the particles in the loop were heavier than the external particles. Expanding the correction functions in the mass splitting, which is now negative, we find:

$$\mathcal{E}_S(r, \kappa)|_{|\vec{p}|\rightarrow 0} \approx \frac{1}{1 + 2 \frac{m_1 |\delta m|}{m_\phi^2}}, \quad (36)$$

$$\mathcal{E}_P(r, \kappa)|_{|\vec{p}|\rightarrow 0} \approx \frac{1}{3} \frac{1}{1 + 2 \frac{m_1 |\delta m|}{m_\phi^2}} \cdot \left(\frac{1 + 3 \cdot 2 \frac{m_1 |\delta m|}{m_\phi^2}}{1 + 2 \frac{m_1 |\delta m|}{m_\phi^2}} \right). \quad (37)$$

The enhancement function \mathcal{E}_S is suppressed more strongly than for positive δm , once $2m_1|\delta m| > m_\phi^2$. The suppression for the P -wave is again weaker than for the S -wave.

Note that the expansions (34), (35), (36) and (37) reproduce the exact corrections rather well as long as the kinetic energy (not the momentum) in the initial state is smaller than the absolute value of the mass splitting, i.e. for $\vec{p}^2 < 2m_1|\delta m|$. For the larger mass splitting shown in Figs. 5b and 5c, $\delta m = 100$ GeV, this remains true for nearly the entire momentum range where the non-relativistic expansion can be trusted.

In summary, when the mass splitting is not vanishing, the correction for small initial momenta is suppressed. This suppression is stronger if the particles in the loop are lighter than the external particles, and always increases with the absolute value of the mass splitting. To

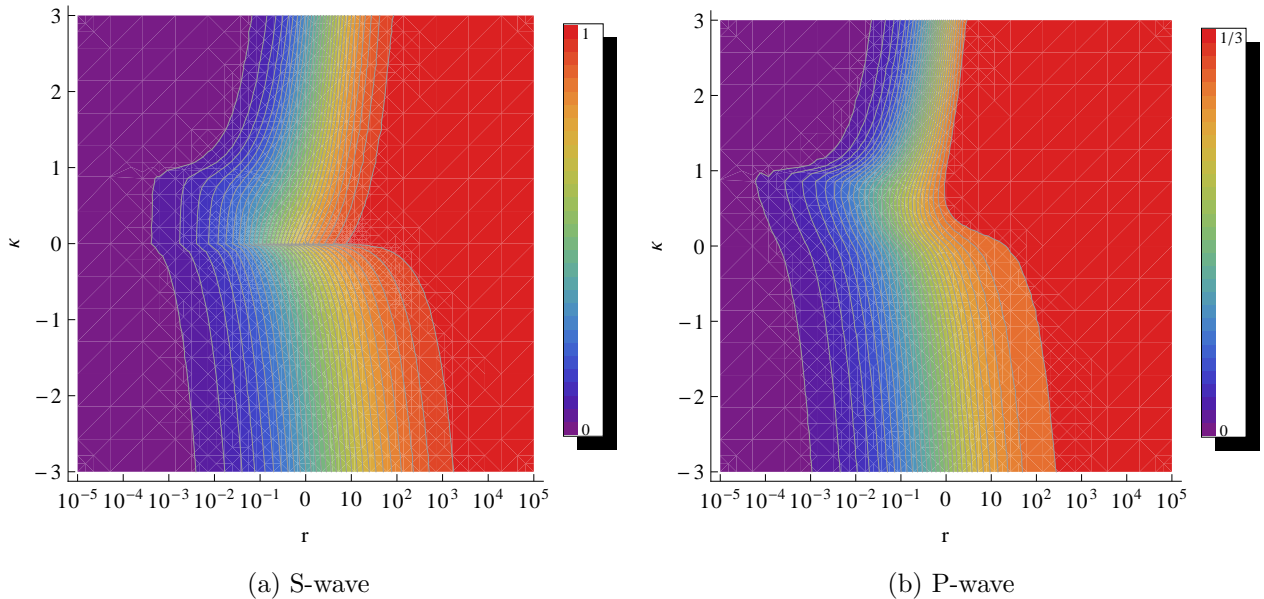


Figure 6: Contour plots of the amplitude enhancement function \mathcal{E}_L in the (κ, r) plane for S -wave (left) and P -wave (right).

illustrate this, we calculate the value of the mass splitting $|\delta m|$ where the correction for $|\vec{p}| \rightarrow 0$ is suppressed to 10% of the correction for $\delta m = 0$. Using formulae (34) and (36) for the S -wave, the corresponding relative mass splitting $|\delta m|/m_1$ is about 20% and 2% for positive δm and negative δm respectively. Intermediate states with yet larger mass splitting can be deemed as relatively unimportant for the correction to the annihilation cross section.

Before concluding this Section, we give contour plots of the amplitude enhancement function \mathcal{E}_L in the (κ, r) -plane, for both S and P partial waves (Fig. 6). In both plots, \mathcal{E}_L is large where r is large and the absolute value of κ is small, corresponding to small three-momentum and small mass splitting. The maximum value of \mathcal{E}_L is 1 and $1/3$ for S - and P -wave, respectively. Recall that the magnitude of the enhancement also depends on the one-loop factor $\alpha m_\chi/m_\phi$. In order to produce a sizeable correction, m_χ/m_ϕ should be large enough while at the same time not too large, in order to keep $\alpha m_\chi/m_\phi$ below 1 so that the one-loop approximation makes sense. In the framework of WIMPs, where the coupling constant is weak, there is still a fairly large range of mass for dark matter particle satisfying this condition.

4 MSSM in the Co-annihilation Region

The results presented so far are model independent. However, in order to gauge the importance of the corrections to the annihilation rates and the current relic density, we need to perform numerical computations in the framework of a specific WIMP model where some particles have masses close to that of the dark matter particle and therefore co-annihilation can happen. In this chapter we choose the Minimal Supersymmetric extension of the Standard Model (MSSM) for this purpose. Before discussing one-loop corrections, we give a brief review of the properties of neutralinos and charginos, as well as the form of the Boltzmann equation we will work with.

We then describe the numerical implementation of the corrections, before presenting numerical results.

4.1 Formalism

In the MSSM the four neutralinos are linear combinations of four different neutral fermionic interaction eigenstates: the bino \tilde{B} , the neutral wino \tilde{W}^0 , and two neutral higgsinos $\tilde{H}_1^0, \tilde{H}_2^0$. These states mix as a result of electroweak gauge symmetry breaking. This mixing can be described by the mass matrix of the four fermions in the basis $(\tilde{B}, \tilde{W}^0, \tilde{H}_1^0, \tilde{H}_2^0)$ [10],

$$\mathcal{M}^0 = \begin{pmatrix} M_1 & 0 & -M_Z s_W c_\beta & M_Z s_W s_\beta \\ 0 & M_2 & M_Z c_W c_\beta & -M_Z c_W s_\beta \\ -M_Z s_W c_\beta & M_Z c_W c_\beta & 0 & -\mu \\ M_Z s_W s_\beta & -M_Z c_W s_\beta & -\mu & 0 \end{pmatrix}. \quad (38)$$

Here, M_1 and M_2 are the bino and wino masses, respectively, and μ is the supersymmetric higgsino mass parameter. The off-diagonal terms, which cause higgsino–gaugino mixing, result from gauge–strength Higgs–higgsino–gaugino interactions, which contribute to the neutralino mass matrix when the Higgs fields attain vacuum expectation values (vevs). s_W is shorthand for $\sin \theta_W$, and c_W, s_β, c_β stand for $\cos \theta_W, \sin \beta$, and $\cos \beta$. Here $\tan \beta$ is the ratio of the vevs of the two Higgs fields. The mass matrix \mathcal{M}^0 is diagonalized by a 4×4 unitary matrix \mathcal{Z} to produce four Majorana neutralino mass eigenstates,

$$\tilde{\chi}_i^0 = \mathcal{Z}_{i1} \tilde{B} + \mathcal{Z}_{i2} \tilde{W}^0 + \mathcal{Z}_{i3} \tilde{H}_1^0 + \mathcal{Z}_{i4} \tilde{H}_2^0. \quad i = 1, 2, 3, 4 \quad (39)$$

Which one of the four neutralinos is the lightest depends on the parameters M_1, M_2, μ and $\tan \beta$. The lightest neutralino can be a good WIMP Dark Matter candidate, if it is stable. This condition is satisfied if the lightest neutralino is also the lightest of all superparticles (LSP) and if R –parity, or a similar symmetry under which particles and superpartners transform differently, is preserved.

The parameters that determine the neutralino mass matrix (38) also appear in the Dirac mass matrix mixing the charged wino and higgsino states. It is given by [10]

$$\mathcal{M}^\pm = \begin{pmatrix} M_2 & \sqrt{2} M_W s_\beta \\ \sqrt{2} M_W c_\beta & \mu \end{pmatrix}. \quad (40)$$

Since the chargino mass matrix is not symmetric, one needs two unitary matrices U, V for its diagonalization, i.e. the left- and right-handed components of the chargino mass eigenstates $\tilde{\chi}_{1,2}^\pm$ mix differently [10].

Co-annihilation between the lightest neutralino and lightest chargino is important whenever⁹ $M_2 < |M_1|, |\mu|$ or $|\mu| < |M_1|, M_2$. In the former case both $\tilde{\chi}_1^0$ and $\tilde{\chi}_1^\pm$ are dominated by their wino components. To good approximation these three states form a triplet under the weak $SU(2)$ gauge symmetry. The tree-level mass difference between the lightest neutralino and chargino is then of order $M_Z^4/M_1 \mu^2$ [13]. This is extremely small ($M_1, \mu \gg M_Z$), and radiative corrections have to be included. If scalars are somewhat heavier than the lighter wino-like

⁹We follow the usual convention where M_2 is real and positive; this can be assured by phase transformations without loss of generality. M_1 and/or μ can then be negative or, in the presence of CP–violation, complex.

states, these corrections amount to about 170 MeV [13], so that the chargino–neutralino mass differences is almost independent of the parameters of the neutralino mass matrix.

In the second scenario, $\tilde{\chi}_1^0$, $\tilde{\chi}_1^\pm$ and $\tilde{\chi}_2^0$ are all dominated by their higgsino components. Up to small corrections, they form two two–component doublets of the $SU(2)$ gauge symmetry, which can be grouped into a single doublet of Dirac fermions. The mass differences are of order of M_Z^2/M_1 , M_Z^2/M_2 [14], which are still small, but much larger than in the wino–dominated case. In the presence of large $\tilde{t}_L - \tilde{t}_R$ mixing radiative corrections to the mass splitting can be of comparable size as the tree–level splitting [14, 15]. However, in the region of parameter space where the thermal relic density of a higgsino–like $\tilde{\chi}_1^0$ has the right magnitude, the relative mass splittings remain quite small even after one–loop corrections. Here we ignore these corrections for simplicity. Note also that in this scenario the mass of the lighter chargino is typically about midway between the masses of $\tilde{\chi}_1^0$ and $\tilde{\chi}_2^0$.

In both cases, other fermionic particles exist whose masses are close to that of the dark matter particle. The coannihilation mechanism becomes important, including the off–diagonal Sommerfeld effect studied in this paper. Recall that the latter effect is very sensitive to the mass splitting, as observed in the previous Section. For wino–like WIMP the mass splitting is so small that it can be neglected in the calculation of the relic density. On the other hand, for higgsino–like states the mass splitting can be significant, although the relative mass splitting $\delta m/|\mu|$ decreases rather quickly with increasing WIMP mass $\simeq |\mu|$.

Another special phenomenon in the case of higgsino dominance is the physical phase between $\tilde{\chi}_1^0$ and $\tilde{\chi}_2^0$. Simply diagonalizing¹⁰ the bottom right 2×2 block (the higgsino sector) of the neutralino matrix \mathcal{M}^0 , one finds that one of the two mass eigenvalues becomes negative, if \mathcal{Z}_{ij} is kept real. One can then multiply the fermion field with apparently negative mass with a factor $i\gamma_5$, leading to a state with positive (i.e., physical) mass. Then the Feynman rules that involve this particular fermion field need to be modified accordingly [16]. It can be cumbersome to keep track of this special fermion field in calculations. The other way is to relinquish the reality constraint on the matrix \mathcal{Z}_{ij} and multiply the row of \mathcal{Z}_{ij} associated with the field with otherwise negative mass by an imaginary unit i . We choose to adopt this convention. As the elements of the mixing matrix \mathcal{Z}_{ij} appear ubiquitously in Feynman rules for vertices involving neutralinos, the physical relative phase can have a significant impact on the Sommerfeld calculation, as we will see later. This phenomenon does not affect the chargino sector, since the two diagonalization matrices U and V allow enough freedom to make all chargino masses positive even if U and V are real, as long as CP is conserved in the chargino sector.

The rest of this Subsection gives a brief review of the formalism of coannihilation calculation that we use, closely following refs.[9] and [17], where further details can be found.

Consider a chain of supersymmetric particles $\tilde{\chi}_i$ ($i = 1, \dots, N$) whose masses are close: $m_1 \leq m_2 \leq \dots \leq m_{N-1} \leq m_N$ ($\tilde{\chi}_1$ is the WIMP). Then the scatterings

$$\tilde{\chi}_i + X \leftrightarrow \tilde{\chi}_j + Y \tag{41}$$

will be frequent enough to maintain the *relative* equilibrium between the densities of these particles even long after they have collectively decoupled from the thermal bath of the standard model particles, provided the mass splitting between the heaviest and the lightest of these

¹⁰The diagonalization of the matrix \mathcal{M}^0 is $\mathcal{M}_0^D = \mathcal{Z}^* \mathcal{M}^0 \mathcal{Z}^{-1}$; see for example Section 9.2 in [10].

sparticles is significantly smaller than m_1 . This implies

$$\frac{n_{\tilde{\chi}_i}}{n} = \frac{n_{\tilde{\chi}_i}^{\text{eq}}}{n^{\text{eq}}}. \quad (42)$$

However, at some time after the decoupling of $\tilde{\chi}_1$ all heavier states will decay into $\tilde{\chi}_1$, which is our dark matter candidate particle. We therefore only need to keep track of the sum of all superparticle densities, $n \equiv \sum_i n_{\tilde{\chi}_i}$. Consequently the Boltzmann equation describing the evolution of the number density of the dark matter particle is augmented from,

$$\frac{dn_{\tilde{\chi}}}{dt} = -3Hn_{\tilde{\chi}} - \langle \sigma_{\text{ann}} v \rangle (n_{\tilde{\chi}}^2 - n_{\tilde{\chi}}^{\text{eq},2}) \quad (43)$$

to,

$$\frac{dn}{dt} = -3Hn - \sum_{i,j=1}^N \langle \sigma_{ij} v_{ij} \rangle (n_{\tilde{\chi}_i} n_{\tilde{\chi}_j} - n_{\tilde{\chi}_i}^{\text{eq}} n_{\tilde{\chi}_j}^{\text{eq}}), \quad (44)$$

where σ_{ij} is the cross section for the annihilation of $\tilde{\chi}_i$ and $\tilde{\chi}_j$ into Standard Model particles and $\langle \dots \rangle$ denotes thermal averaging. Here we have assumed that all $\tilde{\chi}_i$ remain in kinetic equilibrium during the epoch of chemical decoupling; this is usually the case, since elastic scattering of $\tilde{\chi}_i$ particles on SM particles are much more frequent than $\tilde{\chi}_i \tilde{\chi}_j$ annihilation reactions.

The effects of all the coannihilation channels $\tilde{\chi}_i \tilde{\chi}_j \rightarrow XY$ can be encapsulated in a new quantity, the effective cross section σ_{eff} :

$$\langle \sigma_{\text{eff}} v \rangle = \sum_{ij} \langle \sigma_{ij} v_{ij} \rangle \frac{n_{\tilde{\chi}_i}^{\text{eq}} n_{\tilde{\chi}_j}^{\text{eq}}}{n^{\text{eq}} n^{\text{eq}}} \equiv \frac{A}{n_{\text{eq}}^2}. \quad (45)$$

This allows to recast the Boltzmann equation in a succinct way similar to the expression (43) without coannihilation:

$$\frac{dn}{dt} = -3Hn - \langle \sigma_{\text{eff}} v \rangle (n^2 - n_{\text{eq}}^2). \quad (46)$$

Basically, $\langle \sigma_{\text{eff}} v \rangle$ is just a weighted sum of cross sections of many (co-)annihilation processes. The equilibrium total number density n_{eq} in the denominator of the last expression in Eq.(45) is, using the Maxwell-Boltzmann distribution for f_i :

$$n^{\text{eq}} = \frac{T}{2\pi^2} \sum_i g_i m_i^2 K_2\left(\frac{m_i}{T}\right), \quad (47)$$

where g_i is the number of internal degrees of freedom of $\tilde{\chi}_1$. Similarly, the numerator A can be simplified to,

$$A = \frac{g_1^2 T}{4\pi^4} \int_0^\infty dp_{\text{eff}} p_{\text{eff}}^2 W_{\text{eff}} K_1\left(\frac{\sqrt{s}}{T}\right). \quad (48)$$

The functions $K_1(x)$, $K_2(x)$ appearing in Eqs.(47) and (48) are the modified Bessel function of the second kind of order one and two respectively, and p_{eff} is the absolute value of the three-momentum of $\tilde{\chi}_1$ in the center-of-mass frame of the $\tilde{\chi}_1 \tilde{\chi}_1$ pair, so that $s = 4(m_1^2 + p_{\text{eff}}^2)$. Finally,

W_{eff} is the dimensionless effective annihilation rate that contains weighted contributions from every (co-)annihilation channel:

$$W_{\text{eff}} = \sum_{ij} \sqrt{\frac{[s - (m_i - m_j)^2][s - (m_i + m_j)^2]}{s(s - 4m_1^2)}} \frac{g_i g_j}{g_1^2} W_{ij}. \quad (49)$$

The dimensionless (unpolarized) annihilation rate per unit volume W_{ij} is normalized to $2E_i \cdot 2E_j$ and is related to the (unpolarized) cross section via

$$W_{ij} = 4E_i E_j \sigma_{ij} v_{ij}. \quad (50)$$

The square root factor in eq.(49) is understood to imply that the contribution from W_{ij} vanishes if $\sqrt{s} \leq m_i + m_j$.

The remaining task is thus the calculation of the σ_{ij} . These define W_{eff} via Eq.(49), which in turn allows to calculate $\langle \sigma_{\text{eff}} v \rangle$ via Eqs.(45)–(48). The modified Boltzmann equation (46) can then be integrated numerically. This procedure is the basis of numerical packages like `micrOMEGAs` [18, 19] and `DarkSUSY` [20, 21].

4.2 Numerical Implementation

We use `DarkSUSY` [20, 21] to implement our corrections to the (co-)annihilation cross sections, and hence to the predicted $\tilde{\chi}_1^0$ relic density, since it provides separate subroutines (in `FORTRAN`) for the calculation of all helicity amplitudes for any annihilation process one cares to include in the analysis. We saw in Sec. 2 that the Sommerfeld corrections to co-annihilation only factorize on the amplitude level, not on the cross section level, so we need all relevant amplitudes including their phases. Moreover, the discussion of Table 2 showed that we have to keep track of the spins in the initial state; similarly, we saw in Sec. 2.1 that in some cases the sign of interfering amplitudes depends on the spin, or total angular momentum, of the intermediate state.

We see from Eqs.(13) and (19), keeping the finite mass splitting between co-annihilating neutralinos and charginos only in the coefficient κ defined in Eq.(8), that the one-loop corrected (co-)annihilation amplitude into a given final state consisting of two SM particles can be written as

$$A_L^i(|\vec{p}|, p')|_{1\text{-loop}} = A_{0,L}^i(|\vec{p}|, p') + \sum_{j,\phi} c_N \frac{\alpha m_{\tilde{\chi}_1^0}}{m_\phi} \mathcal{E}_L(\kappa(i, j), r(m_\phi)) A_{0,L}^j(|\vec{p}|, p'). \quad (51)$$

Here the index i (j) labels the initial (intermediate) state consisting of two $\tilde{\chi}$ fermions, and A_0^i (A_0^j) is the corresponding tree-level (co-)annihilation amplitude. For a particular initial state i , often more than one kind of intermediate state j can contribute to the one-loop correction via the exchange of some boson ϕ . Moreover, the same intermediate state j might be accessible through the exchange of several different (relatively) light bosons ϕ . The contributions from all possible intermediate states and all possible exchanged bosons should be summed up in Eq.(51) to account for the complete one-loop correction.

Let us illustrate this with a couple of concrete examples. First, consider the annihilation reaction $\tilde{\chi}_i^0 + \tilde{\chi}_j^0 \rightarrow W^+ + W^-$ in the (more complicated) case where the (co-)annihilating states are higgsino-like. This is in fact one of the most important final states. In this scenario we

have to consider all combinations of i and j with $i, j \in \{1, 2\}$. The initial neutralino pair $\tilde{\chi}_i^0 \tilde{\chi}_j^0$ can “rescatter” into $\tilde{\chi}_m^0 \tilde{\chi}_n^0$ via the exchange of a Z or neutral (CP–even) Higgs boson, where in principle again all combinations $m, n \in \{1, 2\}$ have to be taken into account¹¹; or it can change into $\tilde{\chi}_1^+ \tilde{\chi}_1^-$ via the exchange of a W^\pm or charged Higgs boson. In either case the intermediate $\tilde{\chi}_m^0 \tilde{\chi}_n^0$ or $\tilde{\chi}_1^+ \tilde{\chi}_1^-$ state then annihilates into a W^+W^- pair.

As a second example, consider $\tilde{\chi}_i^0 \tilde{\chi}_1^\pm \rightarrow ZW^\pm$ ($i \in \{1, 2\}$), which is one of the dominant co–annihilation reactions. Charge conservation implies that only $\tilde{\chi}_m^0 \tilde{\chi}_1^\pm$ ($m \in \{1, 2\}$) intermediate states can contribute, but these states are accessible both through the exchange of a neutral gauge or Higgs boson coupling $\tilde{\chi}_i^0$ to $\tilde{\chi}_m^0$ and through the exchange of a charged gauge or Higgs boson coupling $\tilde{\chi}_i^0$ to $\tilde{\chi}_1^\pm$.

We square Eq.(51) and sum up the helicities to get the one–loop corrected squared amplitude, which is proportional to the differential cross section:

$$\sum_{h\bar{h}} |A_L^i(|\vec{p}|, p')|_{1\text{-loop}}^2 = \sum_{h\bar{h}} |A_{0,L}^i|^2 + \sum_{j,\phi} c_N \mathcal{E}_L(\kappa(i, j), r(m_\phi)) \sum_{h\bar{h}} \Re e \left(\frac{2\alpha m_{\tilde{\chi}_1^0}}{m_\phi} A_{0,L}^j A_{0,L}^{i*} \right). \quad (52)$$

Here h and \bar{h} are the helicities of the initial particles. This expression shows explicitly that we need the full amplitude information, including all (relative) phases between different amplitudes, in order to calculate the corrections. We insert the result of Eq.(52) back into the subroutine in **DarkSUSY** that computes the relic density.

Note that **DarkSUSY** does not expand the (co–)annihilation cross sections in powers of the initial three–momentum or, equivalently, into partial waves. On the one hand, this allows us to immediately use the (numerical) subroutines of **DarkSUSY** for the calculation of the relic density from the one–loop corrected annihilation cross section; recall that the corrected cross section cannot be cast into the usual form $\sigma = a + bv^2$.

On the other hand, we saw in Sec. 3 that, as in the case without co–annihilation [3, 4, 5] the Sommerfeld corrections differ significantly for S - and P -wave annihilation. For the purpose of computing the correction, we therefore do decompose the amplitudes into S - and P -wave terms by invoking the subroutine that calculates a given helicity amplitude twice, the first time with zero momentum (i.e. for annihilation at rest), the second time with the actual three–momentum in question. The first call obviously gives the constant (momentum–independent) contribution to this amplitude, which we equate with the S -wave contribution; to the accuracy of our calculation in Sec. 2, where we only kept the leading (necessary) powers of initial three–momentum, this identification is exact. The entire three–momentum dependence of the amplitude is then assumed to be from the P -wave contribution, i.e. we assume the amplitude to be linear in the three–momentum when extracting the P -wave contribution by subtracting the result of the first call from that of the second call of the subroutine. This is not quite correct. In general the amplitude will also contain S -wave contributions that depend quadratically on the three–momentum. Our extraction of the P -wave contribution to a given amplitude will therefore be correct only if the S -wave term is suppressed, or, for roughly comparable S - and

¹¹In practice the exchange of Higgs bosons yields very small corrections in the scenarios we consider, since Higgs bosons couple to $\tilde{\chi}$ states only via higgsino–gaugino mixing. Moreover, among the $Z\tilde{\chi}_i^0\tilde{\chi}_j^0$ couplings in the case at hand only the off–diagonal $Z\tilde{\chi}_1^0\tilde{\chi}_2^0$ coupling is sizable. In practice there is therefore only one combination of m, n that contributes significantly for each given combination i, j . However, our numerical analysis also includes all sub–leading contributions.

P -wave contributions, for sufficiently small three-momenta. Fortunately these are precisely the two cases where the P -wave contribution can be expected to be significant. In order to improve on this approximation, one would also have to allow additional factors of three-momentum in the calculation of the loop functions \mathcal{E}_L , which would add further complications without great improvement of accuracy. Note finally that we need this decomposition into S - and P -wave *only* for deciding which of the two loop functions is applicable; otherwise the exact momentum dependence of the amplitudes provided by DarkSUSY is kept.

At this point a warning to users of DarkSUSY might be in order. While performing the numerical calculations described in the following Subsection, we noticed that the predictions of DarkSUSY for the annihilation rates of several channels, including important reactions like $\tilde{\chi}_1^+ + \tilde{\chi}_1 \rightarrow Z + Z$ and $\tilde{\chi}_1^0 + \tilde{\chi}_1^0 \rightarrow W^+ + W^-$, violated unitarity quite badly for large LSP mass. This is illustrated by the black (solid) curve in Fig. 7, which shows $v\sigma(\tilde{\chi}_1^+ \tilde{\chi}_1^- \rightarrow W^+ + W^-)$ as a function of the LSP mass for very small initial three-momentum $|\vec{p}| = 10^{-3}m_{\tilde{\chi}_1^0}$. At such a small value of $|\vec{p}|$ basically only S -wave annihilation contributes. Unitarity dictates that well above all thresholds, the cross section for a fixed partial rate should decrease like $1/s$, i.e. like $1/m_{\tilde{\chi}_1^0}^2$. Instead the original DarkSUSY predicted a cross section that fell for $m_{\tilde{\chi}_1^0} < 1$ TeV, but then started to rise again.¹²

We located the source of the problem to be the unnecessary and erroneous introduction of imaginary parts to the t - and u -channel propagators in the expressions for the relevant amplitudes. Note that in the final states containing two massive gauge bosons the momentum exchanged in the t - or u -channel is always space-like, hence these propagators do not have absorptive parts. After removing these imaginary parts the cross section shows the expected scaling with LSP mass, as shown by the dashed red line in Fig. 7.¹³ Of course, we use this modified version of DarkSUSY for the calculation of the one-loop corrections.

Finally, we note that in order to make sure that the one-loop correction is perturbative, we only consider scenarios where $2\alpha m_{\tilde{\chi}_1^0}/m_\phi \lesssim 1$. We estimate the resulting upper bound on $m_{\tilde{\chi}_1^0}$ by using the weak coupling constant $\alpha_W = \alpha_{\text{em}}(M_Z)/\sin^2\theta_W \simeq 0.034$ and assuming the mediating boson to be W^\pm , which is the lightest boson that can be exchanged by incoming neutralinos. Our corrections should then remain perturbative for WIMP masses up to at least 1.2 TeV.

4.3 Results and Discussion

First we consider the scenario with wino-like LSP. This can e.g. be motivated from scenarios with anomaly mediated supersymmetry breaking, where the gaugino masses are related by

¹²Over the range shown in Fig. 7 the cross section strictly speaking does not violate unitarity, i.e. the annihilation amplitude is still smaller than unity. However, the behavior of the cross section at large LSP mass is clearly pathological, and would indeed lead to true unitarity violation at sufficiently large mass.

¹³Imaginary parts were introduced to regularize the infrared (IR) divergence in reactions like $\tilde{\chi}_1^+ + \tilde{\chi}_1^0 \rightarrow \gamma + H^+$, which occurs for $s \simeq m_{H^+}^2$. In this special situation the photon energy is very small, so the exchanged chargino is nearly on-shell. Introducing an imaginary part for the propagator of this nearly on-shell chargino indeed regularizes this divergence; however, the proper treatment of IR divergences instead requires the calculation of IR divergent one-loop diagrams, leading to an IR finite total result. Since this IR problem is relevant only for very special parameter choices, we kept the original regularization of DarkSUSY for final states containing one scalar and one massless gauge boson.

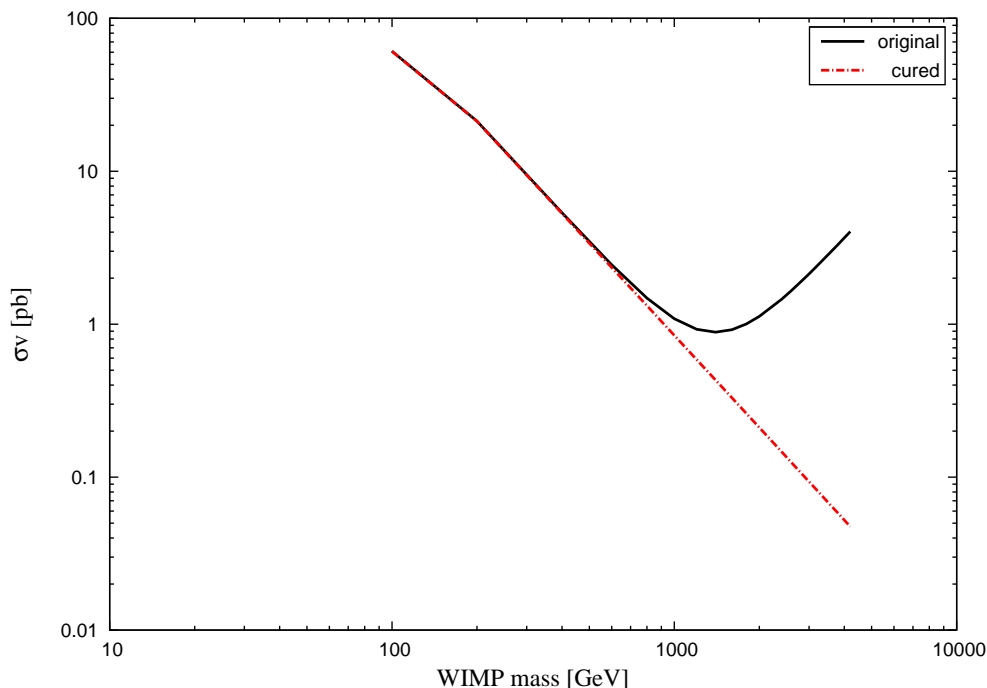


Figure 7: Annihilation rate $v\sigma(\tilde{\chi}_1^+ \tilde{\chi}_1^- \rightarrow W^+W^-)$ for three-momentum $|\vec{p}| = 10^{-3}m_{\tilde{\chi}_1^0}$. The solid (black) curve shows the prediction of the original **DarkSUSY** (version from November 2012), while the dot-dashed (red) curve, which shows the expected $m_{\tilde{\chi}_1^0}^{-2}$ behavior at large masses, is the prediction of the corrected version of **DarkSUSY**; see the text for details.

[22, 23]

$$M_2 \simeq \frac{1}{3}M_1. \quad (53)$$

We consider a wino mass between 100 GeV and 1.4 TeV. The higgsino and sfermion masses are set very high (30 TeV and 6 TeV, respectively), so that higgsino and sfermion exchange diagrams are very strongly suppressed. We assume that there is no flavor mixing in the sfermion sector. Not surprisingly, the spectrum calculator of **DarkSUSY** gives a light neutralino mass range from 100.0 GeV to 1.4 TeV. The original **DarkSUSY** code only calculates the spectrum up to the tree level, which underestimates the chargino-neutralino mass splitting in this case. Because the Sommerfeld correction is sensitive to the mass splitting, we add 0.17 GeV by hand to the chargino masses in the code.

In this scenario, the (co-)annihilation processes that are relevant for the calculation of the LSP relic density are

$$\begin{aligned} \tilde{\chi}_1^0 + \tilde{\chi}_1^0 &\longrightarrow X + Y, \\ \tilde{\chi}_1^+ + \tilde{\chi}_1^- &\longrightarrow X + Y, \\ \tilde{\chi}_1^+ + \tilde{\chi}_1^0 &\longrightarrow X + Y, \quad \text{and its } C\text{-conjugate} \\ \tilde{\chi}_1^+ + \tilde{\chi}_1^+ &\longrightarrow X + Y, \quad \text{and its } C\text{-conjugate} \end{aligned}$$

where X and Y stand for generic standard model particles. Sommerfeld-enhanced W^\pm exchange

can mix the first and second types of processes, whereas reactions of the third and fourth types only receive diagonal corrections, since the total charge in the initial and intermediate state must be the same.

Here we focus on final states with sizeable annihilation rates $\sigma_{ij}v$ and plot the ratios of the corrections due to various intermediate states and the tree-level annihilation rates,

$$R \equiv \frac{\delta\sigma}{\sigma}, \quad (54)$$

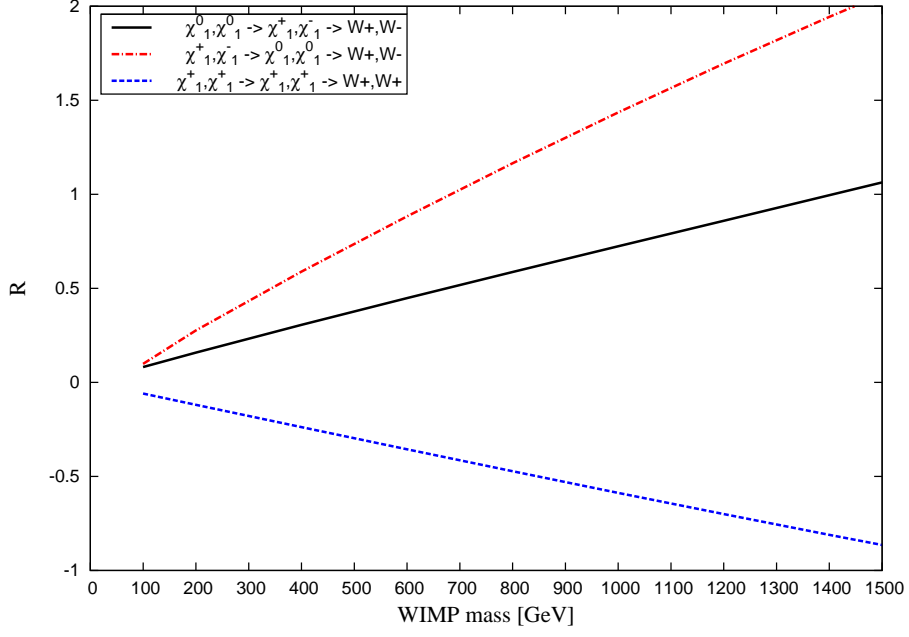
against the WIMP mass. These corrections can be suppressed because of either of the following two reasons. It could be that a given intermediate state is only accessible via suppressed fermion–fermion–boson couplings. Examples are all process $\tilde{\chi}_1^0 + \tilde{\chi}_1^0 \rightarrow \tilde{\chi}_1^0 + \tilde{\chi}_1^0 \rightarrow X + Y$, where the rescattering $\tilde{\chi}_1^0 + \tilde{\chi}_1^0 \rightarrow \tilde{\chi}_1^0 + \tilde{\chi}_1^0$ can be mediated by the Z boson or one of the CP–even neutral Higgs bosons. However, for a pure wino LSP the $\tilde{\chi}_1^0\tilde{\chi}_1^0Z$ coupling is absent for the same reason that the SM doesn’t have a triple– Z coupling, and the $\tilde{\chi}_1^0\tilde{\chi}_1^0(h, H)$ couplings are absent because they require a non–vanishing higgsino component of $\tilde{\chi}_1^0$. Numerically we find $R < 10^{-6}$ in these cases.

Small corrections also result if the given intermediate state has a very small annihilation cross section into the final state under consideration. For example, the correction to $\tilde{\chi}_1^+ + \tilde{\chi}_1^- \rightarrow u + \bar{u}$ annihilation from the $\tilde{\chi}_1^0 + \tilde{\chi}_1^0$ intermediate state is very small since $\tilde{\chi}_1^0 + \tilde{\chi}_1^0 \rightarrow u + \bar{u}$ is suppressed by the very large $m_{\tilde{u}}$ mass we are considering;¹⁴ recall that $\tilde{\chi}_1^0\tilde{\chi}_1^0$ has very suppressed couplings to both the Z and the neutral Higgs bosons, so that the s -channel contributions to $\tilde{\chi}_1^0 + \tilde{\chi}_1^0 \rightarrow u + \bar{u}$ are also very small. In contrast, $\tilde{\chi}_1^+ + \tilde{\chi}_1^- \rightarrow u + \bar{u}$ has sizeable tree-level annihilation rate since γ and Z exchange in the s -channel contribute with full gauge strength. Again we find $R < 10^{-6}$ in this case. Corrections of this size are obviously negligible.

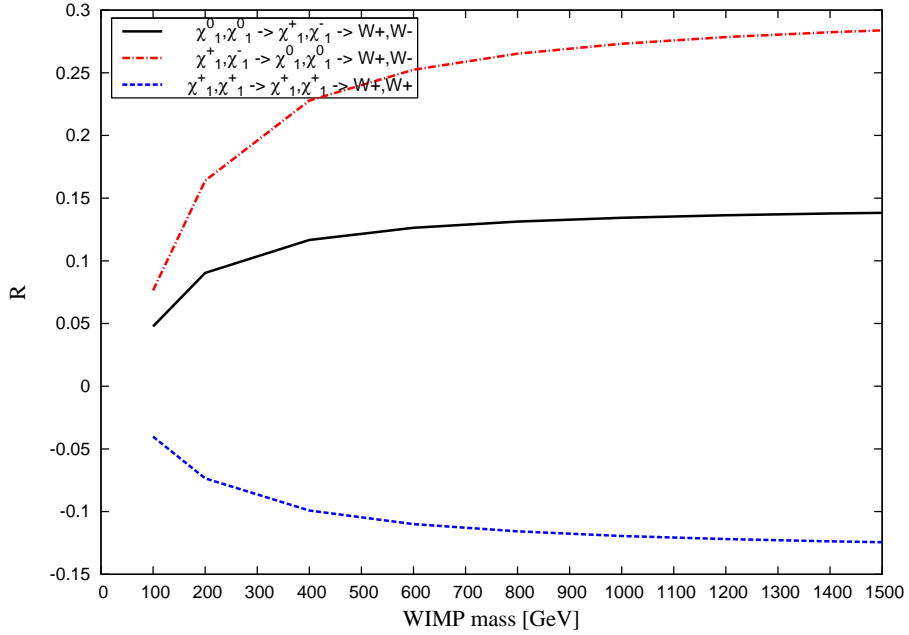
If neither of these two conditions is satisfied, corrections become quite large for large $m_{\tilde{\chi}_1^0}$ and small three-momentum $|\vec{p}|$. As examples we show in Fig. 8 corrections to annihilation into W pair final states for different combinations of initial and intermediate states, and for two values of the three-momentum in the initial state in units of the LSP mass. Note that these figures only include corrections due to the exchange of massive bosons, in particular W^\pm and Z exchange. The $\tilde{\chi}_1^+\tilde{\chi}_1^-$ ($\tilde{\chi}_1^+\tilde{\chi}_1^+$) initial states also contain (diagonal) Sommerfeld corrections due to photon exchange, which have been computed some time ago [24]. The corresponding exact (all-order) corrections are incorporated in our code, but have been suppressed “by hand” when producing the results shown in Fig. 8 in order to show more clearly the effect of one-loop corrections mediated by massive bosons. These photonic all-order corrections will be included later for the calculation of the relic density.

Some features of these plots need to be remarked upon. First, in Fig. 8a the three-momentum is always smaller than the mass of the exchanged boson ($\phi = W$ or Z). As a result, the correction is $\mathcal{O}(\alpha m_{\tilde{\chi}_1^0}/m_\phi)$, and hence increases monotonically with increasing LSP mass. On the other hand, in Fig. 8b the three-momentum can become bigger than m_ϕ . The scale of the correction is then set by $\alpha m_{\tilde{\chi}_1^0}/|\vec{p}|$, which is independent of the LSP mass in Fig. 8 since $|\vec{p}|$ is taken to be a fixed fraction of the LSP mass here. In this case the corrections saturate beyond some value of the LSP mass. This is in accordance with the discussion of Section 3.

¹⁴Even for smaller $m_{\tilde{u}}$ the S -wave contribution to this cross section would be suppressed by a factor $(m_u/m_{\tilde{\chi}_1^0})^2$.



(a) $|\vec{p}| = 0.01 m_{\tilde{\chi}_1^0}$



(b) $|\vec{p}| = 0.33 m_{\tilde{\chi}_1^0}$

Figure 8: Relative size of corrections to annihilation into W pairs from different combinations of wino-like initial and intermediate states: $\tilde{\chi}_1^0 \tilde{\chi}_1^0 \rightarrow \tilde{\chi}_1^+ \tilde{\chi}_1^- \rightarrow W^+ W^-$ (solid, black); $\tilde{\chi}_1^+ \tilde{\chi}_1^- \rightarrow \tilde{\chi}_1^0 \tilde{\chi}_1^0 \rightarrow W^+ W^-$ (dot-dashed, red); and $\tilde{\chi}_1^+ \tilde{\chi}_1^+ \rightarrow \tilde{\chi}_1^+ \tilde{\chi}_1^+ \rightarrow W^+ W^+$ (dashed, blue). The upper (lower) frame is for cms three-momentum $|\vec{p}| = 0.01 m_{\tilde{\chi}_1^0}$ ($|\vec{p}| = 0.33 m_{\tilde{\chi}_1^0}$).

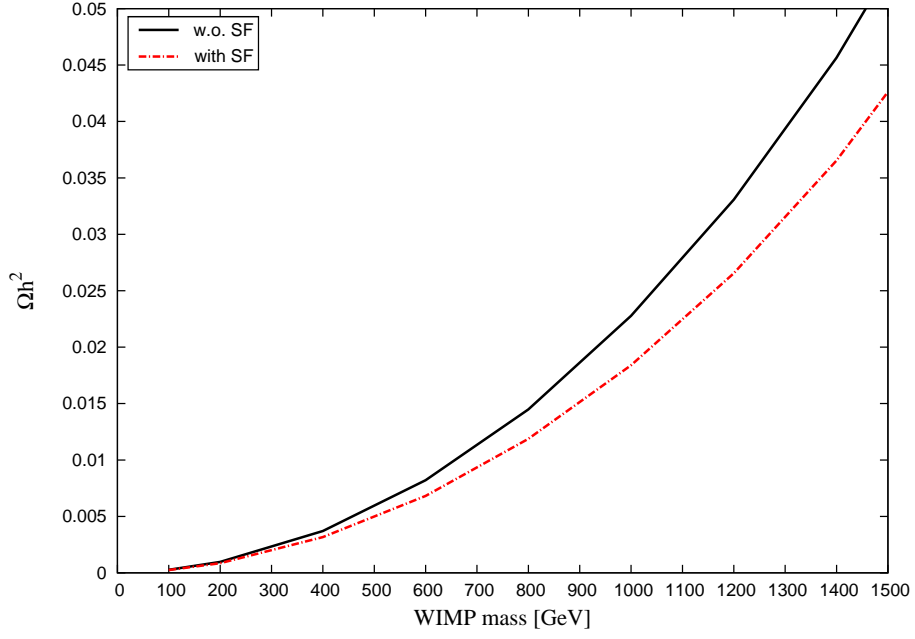
Secondly, while both annihilation reactions into W^+W^- pairs receive positive corrections, the cross section for the annihilation of two positive charginos gets a *negative* correction because the potential between them is repulsive. Note that initial states containing two identical Dirac fermions, rather than a fermion–antifermion pair, lead to “clashing Dirac arrows” in our basic diagram of Fig. 2. As discussed in Sec. 2.1, we treat this using Denner’s convention [11], which gives an explicit minus sign in front of our basic correction of Eq.(2).

We finally note that for large LSP mass the relative correction to $\sigma(\tilde{\chi}_1^+\tilde{\chi}_1^- \rightarrow W^+W^-)$ from the $\tilde{\chi}_1^0\tilde{\chi}_1^0$ intermediate state is about two times bigger than the relative correction to $\sigma(\tilde{\chi}_1^0\tilde{\chi}_1^0 \rightarrow W^+W^-)$ from the $\tilde{\chi}_1^+\tilde{\chi}_1^-$ intermediate state. The $\tilde{\chi}_1^\pm - \tilde{\chi}_1^0$ mass splitting δm is negligible even for $|\vec{p}| = 0.01m_{\tilde{\chi}_1^0}$, because $m_{\tilde{\chi}_1^0}\delta m \ll m_\phi^2$; see Eq.(34). Since both rescatterings proceed via W^\pm exchange, the Sommerfeld correction factors describing the rescattering are nearly the same in both cases. Moreover, while the $\tilde{\chi}_1^+\tilde{\chi}_1^-$ initial state can form a spin triplet (total spin $S = 1$), the $\tilde{\chi}_1^0\tilde{\chi}_1^0$ state has to be a spin singlet ($S = 0$) in the S -wave. This means that the $\tilde{\chi}_1^0\tilde{\chi}_1^0$ intermediate state can only give an S -wave correction to the spin-singlet component of the $\tilde{\chi}_1^+\tilde{\chi}_1^-$ annihilation reaction. In combination, these two facts imply that the numerators of $R(\tilde{\chi}_1^0\tilde{\chi}_1^0 \rightarrow \tilde{\chi}_1^+\tilde{\chi}_1^- \rightarrow W^+W^-)$ and $R(\tilde{\chi}_1^+\tilde{\chi}_1^- \rightarrow \tilde{\chi}_1^0\tilde{\chi}_1^0 \rightarrow W^+W^-)$ are essentially the same. However, the correction to $\tilde{\chi}_1^0\tilde{\chi}_1^0$ annihilation receives an extra factor of 2 (in the S -wave), since the rescattering can produce both a $\tilde{\chi}_1^+\tilde{\chi}_1^-$ and $\tilde{\chi}_1^-\tilde{\chi}_1^+$ intermediate state, whereas the $\tilde{\chi}_1^0\tilde{\chi}_1^0$ intermediate state is unique; see the discussion in Sec. 2.1. On the other hand, the denominators of the two corrections R are quite different, since $\sigma(\tilde{\chi}_1^0\tilde{\chi}_1^0 \rightarrow W^+W^-) \simeq 4\sigma(\tilde{\chi}_1^+\tilde{\chi}_1^- \rightarrow W^+W^-)$. This over-compensates the relative factor of 2 between the two numerators, making the relative correction to chargino annihilation about two times larger than that for neutralino annihilation. Moreover, chargino annihilation also receives sizable “diagonal” corrections from the chargino pair intermediate state, accessible via Z and γ exchange; since no boson has sizable diagonal couplings to two neutralinos in this case, the “diagonal” corrections to LSP annihilation are negligible in this example.

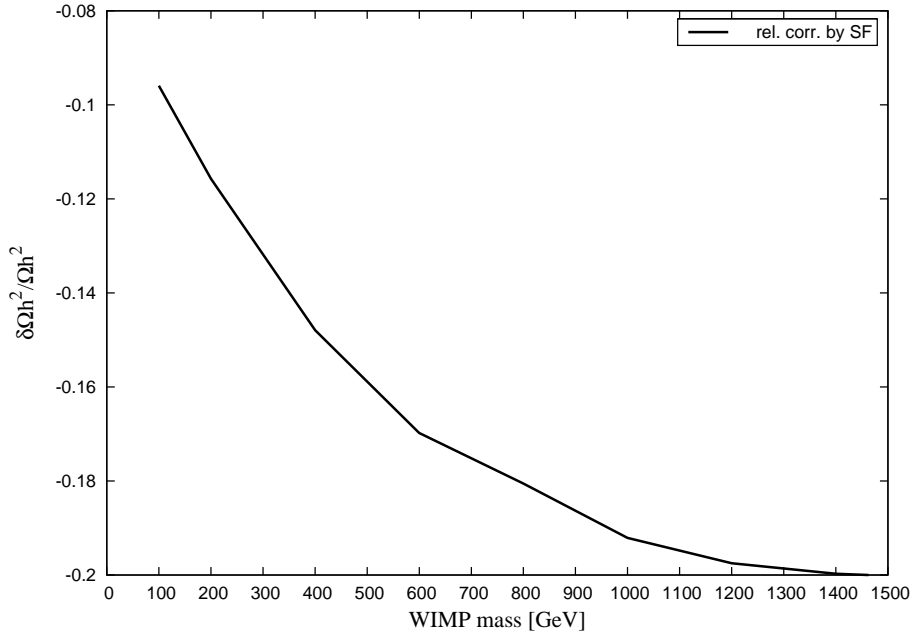
In the next step, we use the corrected annihilation rates to calculate the relic density for LSP mass between 100 GeV and 1.5 TeV. The result is plotted in Fig. 9a, which also shows the tree-level prediction. Evidently the increase of the (co-)annihilation cross sections reduces the relic density. Note that within the range of $\tilde{\chi}$ masses where the correction remains perturbative even for small three-momentum, the thermal relic density in standard cosmology (which is assumed here) is well below the total required Dark Matter density. This problem can be solved by introducing a second Dark Matter component, e.g. an axion or axino [25]. Another possibility is to enhance the expansion rate of the Universe (i.e., the Hubble parameter) during $\tilde{\chi}_1^0$ decoupling, which increases the thermal $\tilde{\chi}_1^0$ relic density [26]; in that case the relative size of the correction to the relic density would still be similar to that shown in Fig. 9a.

This relative correction, $\delta\Omega_{\tilde{\chi}_1^0}/\Omega_{\tilde{\chi}_1^0}$, is plotted in Fig. 9b. We see that the one-loop Sommerfeld correction can be as high as 20%. As expected, the corrections become more important at higher LSP mass. The curve flattens towards large LSP mass, since thermal averaging of the co-annihilation cross sections favors three-momenta $|\vec{p}| \sim 0.1$ to $0.2m_{\tilde{\chi}_1^0}$, which becomes larger than the mass of the exchanged boson $m_\phi = M_W$ or M_Z for large LSP mass; this is the same effect we saw (for slightly higher three-momentum) in Fig. 8.

Next we turn to scenarios with higgsino-like LSP. For simplicity we assume that gaugino



(a) Ωh^2



(b) relative correction to Ωh^2

Figure 9: Thermal LSP relic density with and without the one-loop ‘Sommerfeld’ correction for wino-like LSP. The right panel shows the relative size of the correction to the relic density.

masses unify, which implies for weak-scale masses:

$$M_1 = \frac{1}{2}M_2. \quad (55)$$

In practice this does not matter, since all gaugino masses are set very high, $M_1 = 9.5$ TeV. We consider higgsino masses between 100 GeV and 1.4 TeV, which leads to a very similar range for the LSP mass. Due to the very large gaugino masses, the (tree-level) mass splittings between the higgsino-like states amounts to at most 0.6 GeV. The sfermions are again assumed to be very heavy¹⁵ (15 TeV), and the flavor mixing in the sfermion sector is turned off.

As mentioned in the beginning of this Section, this situation is somewhat more complicated to analyze than scenarios with wino-like LSP, since there are three distinct higgsino-like states, but only two wino-like ones. Correspondingly, the following initial and intermediate states have to be considered: $\tilde{\chi}_1^0\tilde{\chi}_1^0$; $\tilde{\chi}_1^0\tilde{\chi}_2^0$; $\tilde{\chi}_2^0\tilde{\chi}_2^0$; $\tilde{\chi}_1^\pm\tilde{\chi}_1^\mp$; $\tilde{\chi}_1^\pm\tilde{\chi}_1^0$; $\tilde{\chi}_1^\pm\tilde{\chi}_2^0$; $\tilde{\chi}_1^\pm\tilde{\chi}_1^\pm$. Since higgsino-gaugino mixing is again very small, Higgs boson exchange corrections can again be neglected. However, Z boson exchange corrections are now also sizable for neutralino initial states, since the $Z\tilde{\chi}_1^0\tilde{\chi}_2^0$ coupling is large, although the diagonal $Z\tilde{\chi}_i^0\tilde{\chi}_i^0$ ($i = 1, 2$) couplings remain small.

As before, a certain intermediate state only leads to a significant correction to a given annihilation reaction if both the rescattering rate from the initial to the intermediate state and the annihilation rate from the intermediate to the final state are large. Moreover, we again find that for fixed velocity of the annihilating particles, the size of the corrections increases with the LSP mass unless the three-momentum in the initial state is much larger than the mass of the exchanged boson.

One important, qualitatively new feature emerges in this scenario: negative corrections become common, not restricted to annihilation processes of fermions with the same charge. This is possible because of the relative phase between the lightest and the next-to-lightest neutralino.

To see this, consider the limit where $\tilde{\chi}_1^0$ and $\tilde{\chi}_2^0$ are pure higgsino states. For positive μ the neutralino mixing matrix \mathcal{Z} now has the form¹⁶

$$\mathcal{Z} = \begin{pmatrix} 0 & 0 & 1/\sqrt{2} & -1/\sqrt{2} \\ 0 & 0 & i/\sqrt{2} & i/\sqrt{2} \\ \cdots & \cdots & \cdots & \cdots \\ \cdots & \cdots & \cdots & \cdots \end{pmatrix}, \quad (56)$$

In addition, the chargino mixing matrices \mathcal{U} and \mathcal{V} take the form

$$\mathcal{U} = \mathcal{V} = \begin{pmatrix} 0 & 1 \\ 1 & 0 \end{pmatrix}. \quad (57)$$

From these we can calculate the relevant couplings between $\tilde{\chi}$ states and electroweak gauge bosons, using the Feynman rules listed in the Appendix of ref.[10]; for the convenience of the reader we include the relevant rules in Appendix A. It is then not difficult to see that negative corrections can appear in many cases.

¹⁵This means that fermion-sfermion loop contributions to the higgsino mass splitting [14, 15], which we have ignored, will also be small.

¹⁶For $\mu < 0$ the symmetric state is the lighter one, and the i still appears for the second neutralino; i.e. $\mathcal{Z}_{13} = \mathcal{Z}_{14} = -i\mathcal{Z}_{23} = i\mathcal{Z}_{24} = 1/\sqrt{2}$. Moreover a sign then appears in one of the non-vanishing entries of either \mathcal{U} or \mathcal{V} . The subsequent discussion still goes through in this case.

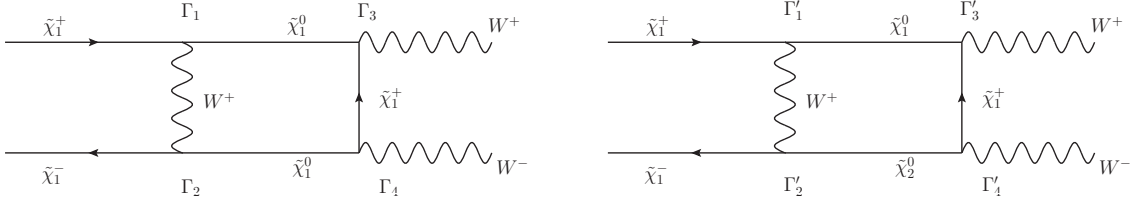


Figure 10: An example where the total correction can be negative. Note that in the right diagram, one of the intermediate $\tilde{\chi}_1^0$ has been replaced by $\tilde{\chi}_2^0$; this gives a relative minus sign between the contributions of these two diagrams.

As a first example, consider corrections to $\tilde{\chi}_1^+ + \tilde{\chi}_1^- \rightarrow W^+ + W^-$ annihilation via neutralino pair intermediate states. Specifically, compare the $\tilde{\chi}_1^0 \tilde{\chi}_1^0$ and $\tilde{\chi}_1^0 \tilde{\chi}_2^0$ intermediate states with t -channel annihilation, as shown in Fig. 10. (The $\tilde{\chi}_1^0 \tilde{\chi}_1^0$ pair basically does not annihilate via an s -channel diagram.) The relative sign between these contributions depends on the products of couplings associated with the four vertices shown in Fig. 10; in contrast to Eq.(2), Γ_i now includes both the coupling strength and the Dirac structure of the corresponding vertex.

Let us begin with the $\tilde{\chi}_1^0 \tilde{\chi}_1^0$ intermediate state. The two vertices Γ_1, Γ_2 describing the rescattering stage are:

$$\Gamma_1 : ig_2 \gamma^\mu (C_{11}^L P_L + C_{11}^R P_R) = ig_2 \gamma^\mu \cdot \left(\frac{1}{2} \right),$$

$$\Gamma_2 : ig_2 \gamma^\nu (C_{11}^{L*} P_L + C_{11}^{R*} P_R) = ig_2 \gamma^\nu \cdot \left(\frac{1}{2} \right).$$

Similarly, the two vertices Γ_3, Γ_4 describing the t -channel annihilation of the intermediate state are:

$$\Gamma_3 : ig_2 \gamma^\rho (C_{11}^L P_L + C_{11}^R P_R) = ig_2 \gamma^\rho \cdot \left(\frac{1}{2} \right),$$

$$\Gamma_4 : ig_2 \gamma^\sigma (C_{11}^{L*} P_L + C_{11}^{R*} P_R) = ig_2 \gamma^\sigma \cdot \left(\frac{1}{2} \right).$$

Now consider the $\tilde{\chi}_1^0 \tilde{\chi}_2^0$ intermediate state. The four corresponding vertices are:

$$\Gamma'_1 : ig_2 \gamma^\mu (C_{11}^L P_L + C_{11}^R P_R) = ig_2 \gamma^\mu \cdot \left(\frac{1}{2} \right),$$

$$\Gamma'_2 : ig_2 \gamma^\nu (C_{21}^{L*} P_L + C_{21}^{R*} P_R) = ig_2 \gamma^\nu \cdot \left(i \frac{1}{2} \right),$$

$$\Gamma'_3 : ig_2 \gamma^\rho (C_{11}^L P_L + C_{11}^R P_R) = ig_2 \gamma^\rho \cdot \left(\frac{1}{2} \right),$$

$$\Gamma'_4 : ig_2 \gamma^\sigma (C_{21}^{L*} P_L + C_{21}^{R*} P_R) = ig_2 \gamma^\sigma \cdot \left(i \frac{1}{2} \right).$$

From these expressions we see that the two intermediate states lead to exactly the same Dirac structure of the vertices [all are vector-like, because the two higgsino doublets form a vector-like representation of $SU(2)$]; moreover, all couplings have the same strength (i.e., absolute value). However, due to the two i factors appearing for the $\tilde{\chi}_1^0\tilde{\chi}_2^0$ intermediate state, the product of couplings for this intermediate state is negative, while it is positive for the $\tilde{\chi}_1^0\tilde{\chi}_1^0$ intermediate state.

A similar analysis shows that the combination of coupling factors for the $\tilde{\chi}_2^0\tilde{\chi}_2^0$ intermediate state is the same as that for the $\tilde{\chi}_1^0\tilde{\chi}_1^0$ intermediate state, while the $\tilde{\chi}_2^0\tilde{\chi}_1^0$ intermediate state contributes with the same product of couplings as the $\tilde{\chi}_1^0\tilde{\chi}_2^0$ intermediate state. In the limit where all mass differences between the charged and neutral higgsinos can be ignored, the total contribution from all four intermediate states thus vanishes!

This may be surprising at first sight, but it can be understood from the observation that in this limit, the higgsinos form a degenerate $SU(2)$ doublet of Dirac fermions. In that case a diagram like those in Fig. 10 does not exist. Start with the incoming $\tilde{\chi}_1^+$. It can emit a W^+ at the first vertex to turn into the neutral Dirac higgsino, which is the lower component of the doublet. However, this lower component cannot emit yet another W^+ at the second vertex, as required in these diagrams, so they do not exist in this limit.

On the other hand, the neutral Dirac higgsino *can* emit a W^- , so a u -channel diagram similar to the ones shown in Fig. 10 should exist in the pure higgsino limit. In our calculations with two distinct neutral Majorana higgsinos, the coupling factors for these u -channel diagrams can be obtained from those for the t -channel by swapping the couplings C in Γ_3 and Γ_4 , taking care to keep track of neutralino indices. This does not change anything for the $\tilde{\chi}_1^0\tilde{\chi}_1^0$ intermediate state, where the same neutralino index appears everywhere. However, for the $\tilde{\chi}_1^0\tilde{\chi}_2^0$ intermediate state, we now get the coupling factors C_{21}^L, C_{21}^R in Γ'_3 without complex conjugation; instead, now C_{11}^{L*} and C_{11}^{R*} appear in Γ'_4 , but these couplings are real. The purely imaginary couplings therefore now contribute $i \times (-i) = 1$, rather than $i \times i = -1$ for the t -channel diagrams. Hence there is no cancellation between the different u -channel diagrams.¹⁷

Fig. 11 shows that the total correction to $\tilde{\chi}_1^+\tilde{\chi}_1^-$ annihilation from neutralino intermediate states is nevertheless negative. The reason is that only intermediate states containing two different neutralinos can annihilate efficiently into SM fermion-antifermion final states via s -channel exchange of a Z boson. The total contribution from these mixed intermediate states is therefore considerably larger in magnitude than the contribution from both intermediate states containing two equal neutralinos. The fact that the $\tilde{\chi}_1^0\tilde{\chi}_2^0$ intermediate state gives a negative correction to $\sigma(\tilde{\chi}_1^+\tilde{\chi}_1^- \rightarrow f\bar{f})$, where f is an SM fermion, can again be understood easily using the notion of Dirac higgsinos: the coupling of the Z boson to neutral and charged higgsinos will then have opposite sign, since their I_3 (weak isospin) values have opposite sign. Note, however, that there are also positive contributions from $\tilde{\chi}_1^+\tilde{\chi}_1^-$ intermediate states, which are not shown in Fig. 11.

Another instance that involves a possibly negative correction occurs in $\tilde{\chi}_1^+\tilde{\chi}_1^0$ annihilation. We compare the intermediate states $\tilde{\chi}_1^+\tilde{\chi}_1^0$ and $\tilde{\chi}_1^+\tilde{\chi}_2^0$, see Fig. 12. We only consider s -channel annihilation in this example. The left diagram then shows the only sizable contribution from $\tilde{\chi}_1^0\tilde{\chi}_1^+$ (or vice versa) intermediate states. We again calculate the three vertex factors in these

¹⁷The Dirac higgsino limit also allows to understand why $\sigma(\tilde{\chi}_1^+\tilde{\chi}_1^+ \rightarrow W^+W^+)$ is very small for higgsino-like LSP, in sharp contrast to the case of wino-like LSP where it is large.

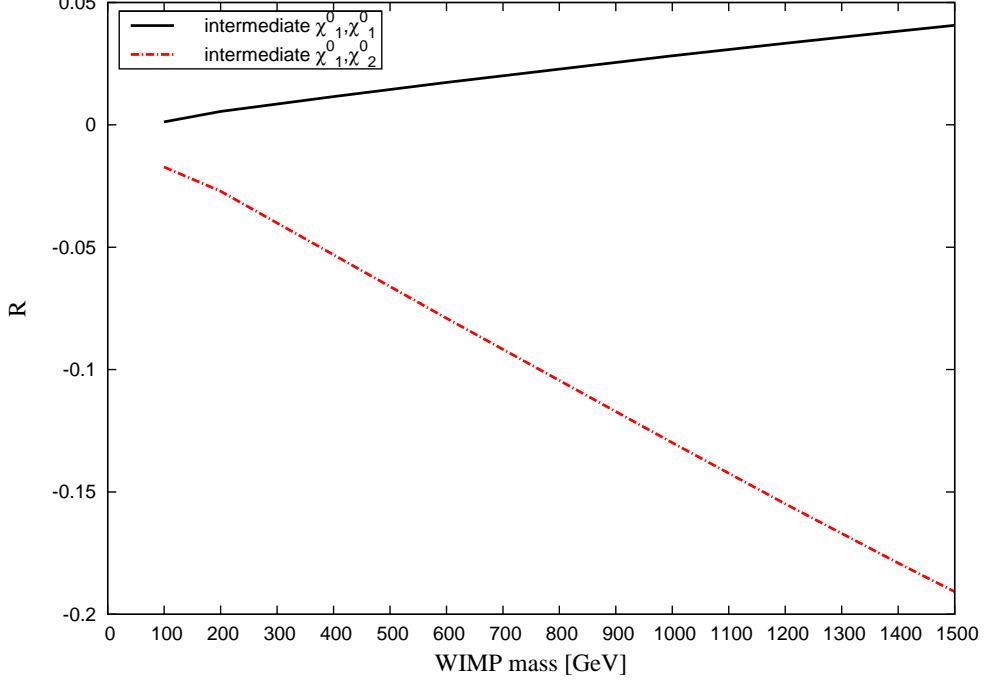


Figure 11: The relative correction to the total annihilation rate of $\tilde{\chi}_1^+ \tilde{\chi}_1^-$, for the $\tilde{\chi}_1^0 \tilde{\chi}_1^0$ (solid, black) and $\tilde{\chi}_1^0 \tilde{\chi}_2^0$ (dashed, red) intermediate states; the contribution from $\tilde{\chi}_2^0 \tilde{\chi}_2^0$ is very similar to that from $\tilde{\chi}_1^0 \tilde{\chi}_1^0$. The contributions from all Standard Model final states have been summed, and $|\vec{p}| = 0.01 m_{\tilde{\chi}_1^0}$.

diagrams. For the left diagram:

$$\begin{aligned}\Gamma_1 &= ig_2 \gamma^\mu (C_{11}^L P_L + C_{11}^R P_R) = ig_2 \gamma^\mu \cdot \left(\frac{1}{2}\right), \\ \Gamma_2 &= ig_2 \gamma^\mu (C_{11}^{R*} P_L + C_{11}^{L*} P_R) = ig_2 \gamma^\mu \cdot \left(\frac{1}{2}\right), \\ \Gamma_0 &= ig_2 \gamma^\mu (C_{11}^R P_L + C_{11}^L P_R) = ig_2 \gamma^\mu \cdot \left(\frac{1}{2}\right).\end{aligned}$$

For the right diagram:

$$\begin{aligned}\Gamma'_1 &= ig_2 \gamma^\mu (C_{21}^L P_L + C_{21}^R P_R) = ig_2 \gamma^\mu \cdot \left(-\frac{i}{2}\right), \\ \Gamma'_2 &= ig_2 \gamma^\mu (C_{11}^{R*} P_L + C_{11}^{L*} P_R) = ig_2 \gamma^\mu \cdot \left(\frac{1}{2}\right), \\ \Gamma'_0 &= ig_2 \gamma^\mu (C_{21}^R P_L + C_{21}^L P_R) = ig_2 \gamma^\mu \cdot \left(-\frac{i}{2}\right).\end{aligned}$$

From Eq.(52) one again finds a relative minus sign between these contributions. In fact, in the pure higgsino limit these contributions will cancel exactly; this can also be understood from the observation that no such diagram can be drawn for neutral Dirac higgsinos.

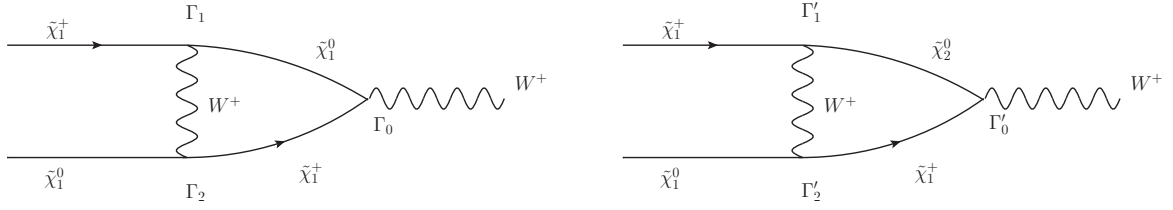


Figure 12: A second example where the total correction can be negative. In the right diagram the intermediate $\tilde{\chi}_1^0$ has been replaced by a $\tilde{\chi}_2^0$, giving a relative minus sign between the contributions from these diagrams.

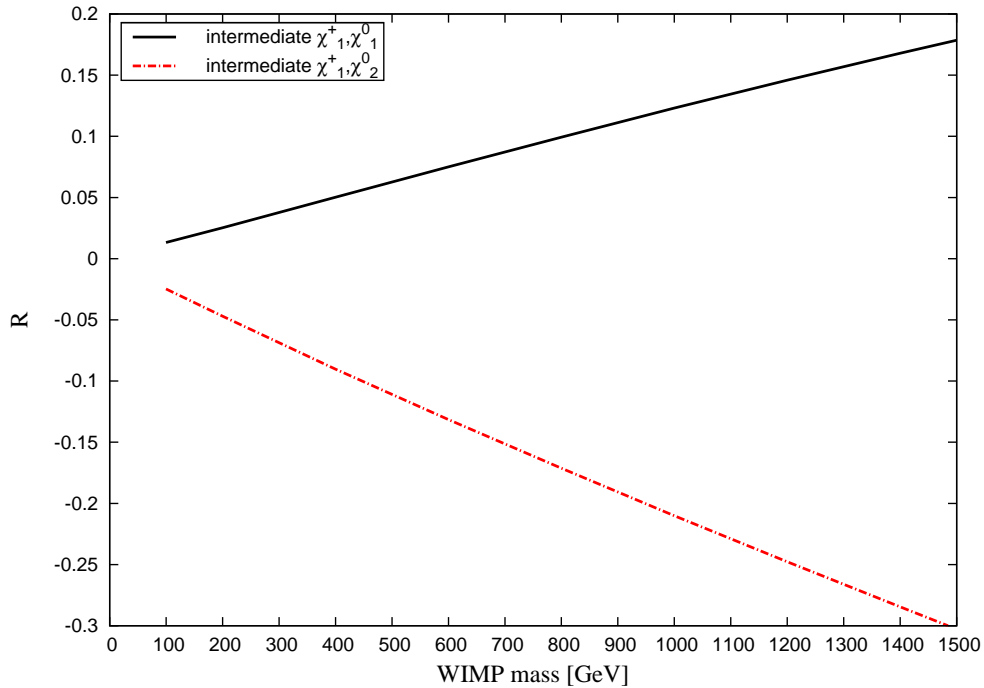


Figure 13: The relative correction to the total annihilation rate of $\tilde{\chi}_1^+ \tilde{\chi}_1^0$, for the $\tilde{\chi}_1^0 \tilde{\chi}_1^+$ (solid, black) and $\tilde{\chi}_2^0 \tilde{\chi}_1^+$ (dashed, red) intermediate states. The contributions from all Standard Model final states have been summed, and $|\vec{p}| = 0.01 m_{\tilde{\chi}_1^0}$.

We see in Fig. 13 that after summing over all SM final states, the negative contributions again win. In this case the two intermediate states shown have very similar annihilation cross sections for all contributing final states. However, the intermediate state containing the heavier neutralino $\tilde{\chi}_2^0$ is enhanced because it is also accessible via Z exchange in the rescattering process, whereas the $\tilde{\chi}_1^0 \tilde{\chi}_1^+$ intermediate state is only accessible via the W exchange diagram shown in Fig. 12.

In fact, the numerical calculation shows that negative corrections occur quite frequently in the co-annihilation of higgsino-like states. For example, $\tilde{\chi}_1^+ \tilde{\chi}_1^-$ states coupled to $\tilde{\chi}_1^0 \tilde{\chi}_2^0$ states,

with either state in the initial and the other in the intermediate state, yields negative corrections. The same is true for $\tilde{\chi}_1^+ \tilde{\chi}_1^0$ coupling to $\tilde{\chi}_1^+ \tilde{\chi}_2^0$, where again either state can be in the initial state.

The cancellation of positive and negative corrections to individual annihilation processes in the end leads to a small correction to the total effective annihilation rate, which can be either positive or negative. As a result, the relic density is slightly enhanced or reduced over the range of the WIMP mass considered, as shown in Fig. 14b. For the correct relic density ($\Omega h^2 \simeq 0.113$), the total one-loop correction turns out to be very small, less than 0.5%. However, this is largely “accidental”, since the corrections for fixed initial, intermediate and/or final state are typically much larger, as shown in the previous figures.

5 Summary and Conclusions

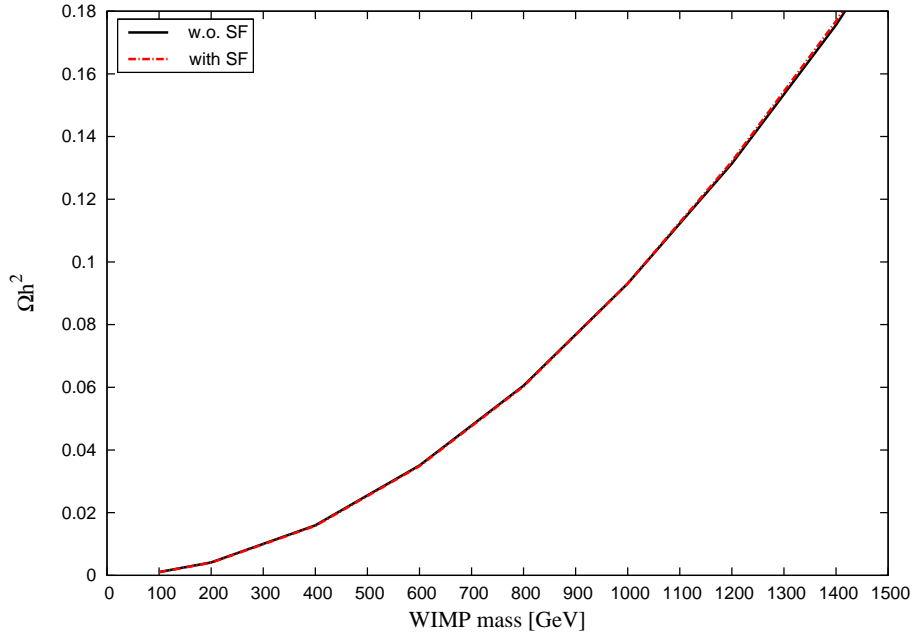
In this paper we have computed enhanced one-loop corrections to the co-annihilation of WIMPs due to the exchange of a light boson in the initial state, treating both S - and P -wave initial states and carefully including the effects from multiple interfering intermediate states (so-called “Sommerfeld” corrections). The ultimate goal is a more accurate calculation of the thermal WIMP relic density.

In Sec. 2 we extended the formalism of ref.[5] to deal with the “multistate” Sommerfeld effect, where the particles in the intermediate state could be different from those in the initial state, although the mass splitting should be relatively small. Since co-annihilation of the slightly heavier partners of the WIMPs also needs to be treated, we considered cases where the intermediate state is lighter or heavier than the initial state, in addition to the usual case where the initial and intermediate states have the same masses. We found exact analytical expressions for the functions describing the one-loop corrections for all three cases; these supercede the numerical fits found in ref.[5] for the case of equal masses.

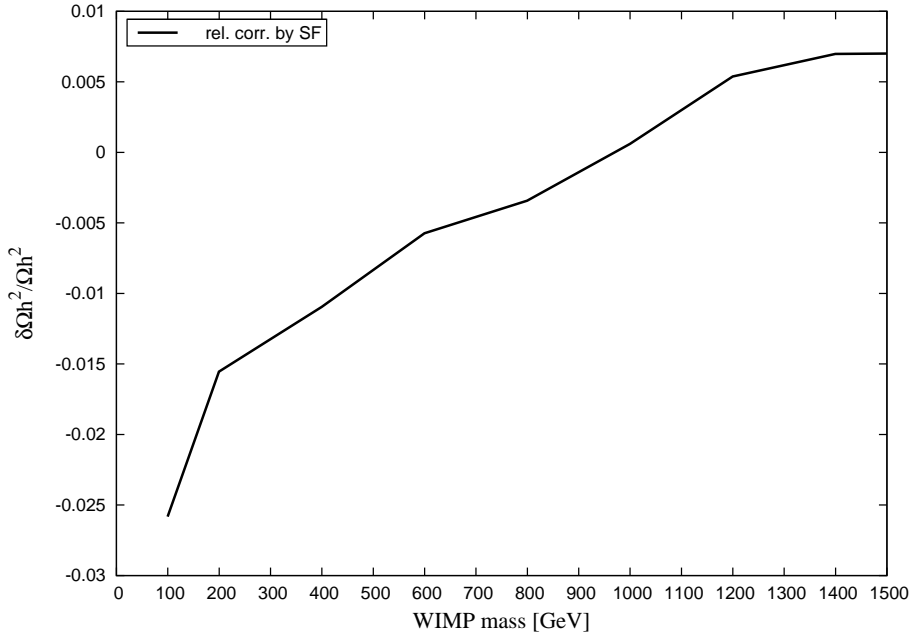
As the intermediate state particles are almost on-shell, the boson exchange can still be regarded as a rescattering reaction, which however is in general off-diagonal. As a result, the corrections no longer factorize at the level of the annihilation cross sections, although they do factorize at the level of the amplitude. The existence of several interfering intermediate states can lead to additional complications, as discussed in Sec. 2.1. In the final subsection of Sec. 2 we showed that the exchange of a light fermion does not lead to enhanced corrections to the co-annihilation of a boson with a (heavy) fermion.

The dependence of the loop functions on various quantities is discussed in Sec. 3. We found that the mass splitting δm_χ between co-annihilating particles affects the loop functions significantly whenever $m_\chi |\delta m_\chi| \gtrsim m_\phi^2$, where m_χ is the WIMP mass and m_ϕ is the mass of the exchanged boson. For very small external three-momentum a non-vanishing mass splitting always reduces the correction, the effect being more pronounced for annihilation from the S -wave. However, if the intermediate state is heavier than the initial state, the loop function develops a peak where the center-of-mass frame energy equals exactly the total mass of the intermediate state.

In Sec. 4 we applied this formalism to the calculation of the relic density of the lightest neutralino in the MSSM. In that case co-annihilation is generic if the LSP is either wino- or higgsino-like. In the former case the co-annihilation with the lightest chargino has to be considered. We found that most corrections are positive, i.e. they reduce the relic density



(a) Ωh^2



(b) relative correction to Ωh^2

Figure 14: Current relic density with and without the one-loop “Sommerfeld” correction for higgsino-like LSP. The right panel shows the relative size of the correction.

even further. The correct thermal relic density is then reached for a range of WIMP masses where the one-loop corrections become so large that they need to be re-summed [2]. For higgsino-like LSP, the two lightest neutralinos and the lighter chargino all contribute in various

co-annihilation reactions. In this case many corrections turn out to be negative. We saw that in many cases this can be understood in the limit of exact higgsino LSP, in which case the two lightest neutralinos can be grouped into a neutral Dirac higgsino, which is an $SU(2)$ partner of the lighter chargino. We found that in this case the total correction to the thermal relic density happens to cancel to good approximation, even though corrections to specific initial and/or final states can be quite sizable.

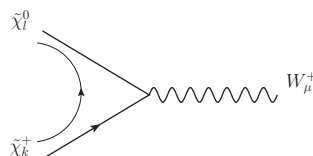
This paper thus completes the model-independent treatment of one-loop ‘‘Sommerfeld’’-enhanced corrections to WIMP annihilation, and at the same time adds to the growing literature on potentially large corrections to the (co-)annihilation of supersymmetric neutralinos.

Acknowledgments

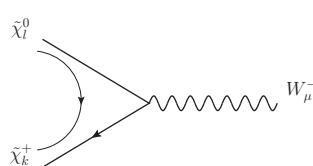
We thank Ju Min Kim and Keiko Nagao for collaboration in the early stages of this research. This work was supported by the TR33 ‘‘The Dark Universe’’ funded by the Deutsche Forschungsgemeinschaft. JG also thanks the Bonn-Cologne Graduate School for support.

A MSSM Vertices

Here we list some Feynman rules for vertex factors in the MSSM used in our calculations. They are taken from Ref.[10] and adapted to Denner’s convention [11].



$$ig_2\gamma_\mu(C_{lk}^L P_L + C_{lk}^R P_R), \quad (58)$$



$$ig_2\gamma_\mu(C_{lk}^{L*} P_L + C_{lk}^{R*} P_R), \quad (59)$$

$$C_{lk}^L = Z_{l2}\mathcal{V}_{k1}^* - \frac{1}{\sqrt{2}}Z_{l4}\mathcal{V}_{k2}^*,$$

$$C_{lk}^R = Z_{l2}^*\mathcal{U}_{k1} + \frac{1}{\sqrt{2}}Z_{l3}^*\mathcal{U}_{k2},$$

$$k = 1, 2; l = 1, 2, 3, 4.$$

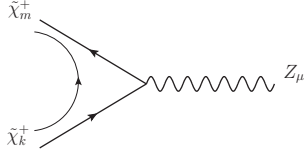
Figure 15: $\tilde{\chi}^+\tilde{\chi}^0W^+$ vertices.



$$-ie\gamma_\mu\delta_{mk} \quad (60)$$

Figure 16: $\tilde{\chi}^+\tilde{\chi}^+\gamma$ vertex.

$$i \frac{g_2}{c_W} \gamma_\mu (O_{mk}^L P_L + O_{mk}^R P_R), \quad (61)$$



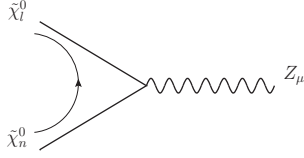
$$O_{mk}^L = -\mathcal{V}_{m1} \mathcal{V}_{k1}^* - \frac{1}{2} \mathcal{V}_{m2} \mathcal{V}_{k2}^* + \delta_{mk} s_W^2,$$

$$O_{mk}^R = -\mathcal{U}_{m1}^* \mathcal{U}_{k1} - \frac{1}{2} \mathcal{U}_{m2}^* \mathcal{U}_{k2} + \delta_{mk} s_W^2,$$

$$m, k = 1, 2.$$

Figure 17: $\tilde{\chi}^+ \tilde{\chi}^+ Z$ vertex.

$$i \frac{g_2}{c_W} \gamma_\mu (N_{ln}^L P_L + N_{ln}^R P_R), \quad (62)$$



$$N_{ln}^L = \frac{1}{2} (-\mathcal{Z}_{l3} \mathcal{Z}_{n3}^* + \mathcal{Z}_{l4} \mathcal{Z}_{n4}^*),$$

$$N_{ln}^R = -(N_{ln}^L)^*,$$

$$l, n = 1, 2, 3, 4.$$

Figure 18: $\tilde{\chi}^0 \tilde{\chi}^0 Z$ vertex.

References

- [1] **WMAP Collaboration**, E. Komatsu *et al.*, “Five-Year Wilkinson Microwave Anisotropy Probe (WMAP) Observations: Cosmological Interpretation,” *Astrophys. J. Suppl.* **180** (2009) 330, [arXiv:0803.0547 \[astro-ph\]](#).
- [2] J. Hisano, S. Matsumoto, and M. M. Nojiri, “Explosive dark matter annihilation,” *Phys. Rev. Lett.* **92** (2004) 031303, [arXiv:hep-ph/0307216 \[hep-ph\]](#); J. Hisano, S. Matsumoto, M. M. Nojiri and O. Saito, “Non-perturbative effect on dark matter annihilation and gamma ray signature from galactic center”, *Phys. Rev.* **D71** (2005) 063528, [hep-ph/0412403](#).
- [3] S. Cassel, “Sommerfeld factor for arbitrary partial wave processes,” *J. Phys.* **G37** (2010) 105009, [arXiv:0903.5307 \[hep-ph\]](#).
- [4] R. Iengo, “Sommerfeld enhancement: General results from field theory diagrams,” *JHEP* **0905** (2009) 024, [arXiv:0902.0688 \[hep-ph\]](#).
- [5] M. Drees, J. M. Kim, and K. Nagao, “Potentially Large One-loop Corrections to WIMP Annihilation,” *Phys. Rev.* **D81** (2010) 105004, [arXiv:0911.3795 \[hep-ph\]](#).
- [6] T. R. Slatyer, “The Sommerfeld enhancement for dark matter with an excited state,” *JCAP* **1002** (2010) 028, [arXiv:0910.5713 \[hep-ph\]](#).

- [7] A. Hryczuk, R. Iengo, and P. Ullio, “Relic densities including Sommerfeld enhancements in the MSSM,” *JHEP* **1103** (2011) 069, [arXiv:1010.2172 \[hep-ph\]](#).
- [8] M. Beneke, C. Hellmann and P. Ruiz-Femenia, “Non-relativistic pair annihilation of nearly mass degenerate neutralinos and charginos I. General framework and S-wave annihilation”, [arXiv:1210.7928 \[hep-ph\]](#).
- [9] K. Griest and D. Seckel, “Three exceptions in the calculation of relic abundances,” *Phys. Rev.* **D43** (1991) 3191.
- [10] M. Drees, R. Godbole, and P. Roy, *Theory and phenomenology of sparticles: An account of four-dimensional N=1 supersymmetry in high energy physics*, World Scientific (2004).
- [11] A. Denner, H. Eck, O. Hahn, and J. Kublbeck, “Compact Feynman rules for Majorana fermions,” *Phys. Lett.* **B291** (1992) 278; and “Feynman rules for fermion number violating interactions,” *Nucl. Phys.* **B387** (1992) 467.
- [12] J.R. Ellis, T. Falk and K.A. Olive, “Neutralino - Stau coannihilation and the cosmological upper limit on the mass of the lightest supersymmetric particle”, *Phys. Lett.* **B444** (1998) 367, [hep-ph/9810360](#);
J.R. Ellis, T. Falk, K.A. Olive and M. Srednicki, “Calculations of neutralino-stau coannihilation channels and the cosmologically relevant region of MSSM parameter space”, *Astropart. Phys.* **13** (2000) 181, Erratum-ibid. **15** (2001) 413, [hep-ph/9905481](#);
M.E. Gomez, G. Lazarides and C. Pallis, “Yukawa unification, $b \rightarrow s\gamma$ and Bino-Stau coannihilation”, *Phys. Rev.* **D61** (2000) 123512, [hep-ph/9907261](#).
- [13] T. Gherghetta, G.F. Giudice and J.D. Wells, “Phenomenological consequences of supersymmetry with anomaly induced masses”, *Nucl. Phys.* **B559** (1999) 27, [hep-ph/9904378](#).
- [14] G.F. Giudice and A. Pomarol, “Mass degeneracy of the Higgsinos”, *Phys. Lett.* **B372** (1996) 253, [hep-ph/9512337](#)
- [15] M. Drees, M.M. Nojiri, D.P. Roy and Y. Yamada, “Light Higgsino dark matter”, *Phys. Rev.* **D56** (1997) 276, Erratum-ibid. **D64** (2001) 039901, [hep-ph/9701219](#).
- [16] H. Baer and X. Tata, “Weak scale supersymmetry: From superfields to scattering events”, Cambridge University Press (2006).
- [17] J. Edsjo and P. Gondolo, “Neutralino relic density including coannihilations,” *Phys. Rev.* **D56** (1997) 1879–1894, [arXiv:hep-ph/9704361 \[hep-ph\]](#).
- [18] G. Belanger *et al.*, “Indirect search for dark matter with micrOMEGAs2.4,” *Comput. Phys. Commun.* **182** (2011) 842, [arXiv:1004.1092 \[hep-ph\]](#).
- [19] G. Belanger, F. Boudjema, A. Pukhov, and A. Semenov, “MicrOMEGAs 2.0: A Program to calculate the relic density of dark matter in a generic model,” *Comput. Phys. Commun.* **176** (2007) 367, [arXiv:hep-ph/0607059 \[hep-ph\]](#).
- [20] P. Gondolo *et al.*, “DarkSUSY: Computing supersymmetric dark matter properties numerically,” *JCAP* **0407** (2004) 008, [arXiv:astro-ph/0406204](#).

- [21] P. Gondolo, J. Edsjo, P. Ullio, L. Bergstrm, M. Schelke, E. Baltz, T. Bringmann, and G. Duda, “Darsusy home page.” <http://www.darksusy.org>.
- [22] L. Randall and R. Sundrum, “Out of this world supersymmetry breaking,” *Nucl. Phys.* **B557** (1999) 79–118, [arXiv:hep-th/9810155](https://arxiv.org/abs/hep-th/9810155) [hep-th].
- [23] G. F. Giudice, M. A. Luty, H. Murayama, and R. Rattazzi, “Gaugino mass without singlets”, *JHEP* **9812** (1998) 027, [arXiv:hep-ph/9810442](https://arxiv.org/abs/hep-ph/9810442) [hep-ph].
- [24] C. Itzykson and J.B. Zuber, “Quantum Field Theory”, McGraw–Hill (1985); L.D. Landau and E.M. Lifshitz, “Quantum Mechanics”, Pergamon Press (1977).
- [25] M. Tegmark, A. Aguirre, M. Rees and F. Wilczek, “Dimensionless constants, cosmology and other dark matters”, *Phys. Rev.* **D73** (2006) 023505, [astro-ph/0511774](https://arxiv.org/abs/astro-ph/0511774); H. Baer, R. Dermisek, S. Rajagopalan and H. Summy, “Neutralino, axion and axino cold dark matter in minimal, hypercharged and gaugino AMSB”, *JCAP* **1007** (2010) 014, [arXiv:1004.3297](https://arxiv.org/abs/1004.3297) [hep-ph]; H. Baer, A. Lessa and W. Sreethawong, “Coupled Boltzmann calculation of mixed axion/neutralino cold dark matter production in the early universe”, *JCAP* **1201** (2012) 036, [arXiv:1110.2491](https://arxiv.org/abs/1110.2491) [hep-ph].
- [26] R. Catena, N. Fornengo, A. Masiero, M. Pietroni and F. Rosati, “Dark matter relic abundance and scalar - tensor dark energy”, *Phys. Rev.* **D70** (2004) 063519, [astro-ph/0403614](https://arxiv.org/abs/astro-ph/0403614); M. Drees, H. Iminniyaz and M. Kakizaki, “Constraints on the very early universe from thermal WIMP dark matter”, *Phys. Rev.* **D76** (2007) 103524, [arXiv:0704.1590](https://arxiv.org/abs/0704.1590) [hep-ph].